Pharmacological Research 211 (2025) 107545

Contents lists available at ScienceDirect

Pharmacological Research

journal homepage: www.elsevier.com/locate/yphrs

Modulation of the endocannabinoid system by (S)-ketamine in an animal model of depression

Nicole R. Silva [a,b], Shokouh Arjmand [b], Luana B. Domingos [a,b], Adriano M. Chaves-Filho [d,f], Melina Mottin [e], Caroline C. Real [b,c], Anna L. Waszkiewicz [b], Pedro H. Gobira [b], Alessio Nicola Ferraro [a], Anne M. Landau [b,c], Carolina H. Andrade [e], Heidi K. Müller [b], Gregers Wegener [b], Sâmia R.L. Joca [a,b,*]

[a] Department of Biomedicine, Aarhus University, Denmark
[b] Translational Neuropsychiatry Unit, Aarhus University, Denmark
[c] Department of Nuclear Medicine and PET Center, Aarhus University and Hospital, Denmark
[d] Division of Medical Sciences, University of Victoria, Canada
[e] Laboratory for Molecular Modeling and Drug Design (LabMol), Faculdade de Farmácia, Universidade Federal de Goiás, Brazil
[f] Neuropharmacology Laboratory, Drug Research and Development Center, Faculty of Medicine, Universidade Federal do Ceará, Brazil

ARTICLE INFO

Keywords:
S-Ketamine
Flinders sensitive line
Endocannabinoids
Lipidome

ABSTRACT

Ketamine (KET) is recognized as rapid-acting antidepressant, but its mechanisms of action remain elusive. Considering the role of endocannabinoids (eCB) in stress and depression, we investigated if S-KET antidepressant effects involve the regulation of the eCB system using an established rat model of depression based on selective breeding: the Flinders Sensitive Line (FSL) and their controls, the Flinders Resistant Line (FRL). S-KET (15 mg/kg) effects were assessed in rats exposed to the open field and forced swimming test (FST), followed by analysis of the eCB signaling in the rat prefrontal cortex (PFC), a brain region involved in depression neurobiology. Changes in eCB receptors and enzymes were assessed at mRNA and protein levels (qPCR and western blot), CB1 binding ([^{3}H]SR141716A autoradiography) and endocannabinoid content (lipidomics). The results demonstrated that the depressive behavior in FSL was negatively correlated with 2-AG levels, which were restored upon acute S-KET treatment. Although S-KET decreased CB1 and FAAH gene expression in FSL, there were no significant changes at protein levels. [^{3}H]SR141716A binding to CB1 receptors was increased by S-KET and *in silico* analysis suggested that it binds to CB1, CB2, GPR55 and FAAH. Overall, S-KET effects correlated with an increased endocannabinoid signaling in the PFC, but systemic treatment with rimonabant failed to block its behavioral effects. Altogether, our results indicate that **S**-KET facilitates eCB signaling in the PFC of FSL. The inability of rimonabant to block the antidepressant effect of S-KET highlights the complexity of its interaction with the ECS, warranting further investigation into the molecular pathways.

Abbreviations: 2S,6S-HNK, 2S,6S-hydroxynorketamine; 2-AG, 2-arachidonoylglycerol; AEA, N-arachidonoyl ethanolamide and; AMPARs, α-amino-3-hydroxy-5-methyl-4-isoxazole-propionic acid receptors; BDNF, Brain-derived neurotrophic factor; CaMKII, Calmodulin kinase II; CB1, Cannabinoid receptors 1; CB2, Cannabinoid receptors 2; DAGL, Diacylglycerol lipases; DHA-EA, Docosahexaenoyl-Ethanolamide; ECL2, Extracellular loop 2; ECS, Endocannabinoid system; EPA-EA, Eicosapentaenoyl-Ethanolamide; FABP5, Fatty Acid Binding Protein 5; FRL, Flinders Resistant Line; FSL, Flinders Sensitive rat Line; FST, Forced Swimming Test; FAAH, Fatty acids amide hydrolase; GPR55, G protein-coupled receptor 55; HI, High immobility; IBB, Interception blocking buffer; KET, Ketamine; LE, Ligand efficiency; LI, Low immobility; Linoleoyl-EA, Linoleoyl-Ethanolamide; MAGL, Monoacylglycerol lipase; MDD, Major depressive disorder; MPFC, Medial prefrontal cortex; NAPE-PLD, N-acyl-phosphatidylethanolamine-hydrolyzing phospholipase D; NMDARs, N-methyl-D-aspartate receptors; OFT, Open field test; Oleoyl-EA, Oleoyl-Ethanolamide; PDB, Protein data bank; PEA, Palmitoyl-Ethanolamide PEA; PFC, Prefrontal cortex; BLA, Basolateral amygdala'; Plddt, Local Distance Difference Test; PLIP, Protein-ligand interaction profiler; RIMO, Rimonabant hydrochloride; RMSD, Root mean square deviation; RT-qPCR, Real Time quantitative PCR; Sal, Saline; S-NORK, S-norketamine; SP, Standard-precision; TrkB, Tropomyosin-related kinase B; TRPV1, Transient receptor potential vanilloid 1; VMD, Visual Molecular Dynamics.

* Correspondence to: Department of Biomedicine, Aarhus University, Aarhus 8000, Denmark.
E-mail address: sjoca@biomed.au.dk (S.R.L. Joca).

https://doi.org/10.1016/j.phrs.2024.107545
Received 30 August 2024; Received in revised form 8 December 2024; Accepted 9 December 2024
Available online 10 December 2024

1. Introduction

Major depressive disorder (MDD) is one of the most prevalent and incapacitating psychiatric disorders [1,2]. It has a heterogeneous clinical presentation, most likely reflecting the complex interplay between polygenic risk factors and exposure to adverse life experiences, such as stress [3–5]. The pharmacological treatment of MDD is not optimal due to several limitations, including delayed onset of therapeutic effects, low remission rates, and high number of patients who are partial responders or non-responders [6–10]. Focused targeting of monoaminergic neurotransmission by classical therapies may contribute to such therapeutic limitations, underscoring the importance of exploring the role of other neurotransmitter systems in MDD and the antidepressant effect [11].

A paradigm shift for MDD treatment was introduced when rapid and sustained antidepressant effects were reported after intravenous Ketamine (KET) administration in MDD patients, which was consistently replicated by other human and animal studies [12–14]. The molecular mechanisms behind KET's rapid antidepressant effect seem to involve multiple targets, with a central participation of glutamatergic neurotransmission [13,15], known to be dysfunctional in MDD [16]. Briefly, KET seems to block NMDAR receptors in GABAergic interneurons in the prefrontal cortex (PFC), thereby disinhibiting local neuronal firing, which subsequently activates post-synaptic AMPAR [17]. AMPAR activation triggers the rapid release of brain-derived neurotrophic factor (BDNF) and subsequent tropomyosin-related kinase B (TrkB) activation, especially in the medial prefrontal cortex (mPFC) [18,19], restoring the dysfunctional neuronal signaling and synaptic plasticity in MDD [20]. KET can also regulate serotonin neurotransmission [21,22] and bind to TrkB [23], thus revealing a multi-targetd and complex pharmacology behind its antidepressant action.

Despite recent evidence suggesting that the rewarding and antinociceptive effects of KET involve the endocannabinoid system (ECS) [24,25], it is not known whether this mechanism is also involved in its antidepressant effect. The ECS is comprised of the main endogenous ligands N-arachidonoyl ethanolamide (AEA) and 2-arachidonoylglycerol (2-AG); the cannabinoid receptors, CB1 and CB2, among others (e.g. G protein-coupled receptor 55 - GPR55); synthesizing (N-acyl-phosphatidylethanolamine-hydrolyzing phospholipase D - NAPE-PLD and Diacylglycerol lipases - DAGL) and degrading enzymes (Fatty acids amide hydrolase - FAAH and Monoacylglycerol lipase - MAGL) [26]. Interestingly, lower serum levels of 2-AG and/or AEA have been described in depressed patients and in the brain of rodents exposed to stress models of depression [27–30]. In line with those observations, genetic and pharmacological studies have shown that compromised CB1 signaling increases the risk of depression [31–33] and impairs the response to monoaminergic antidepressants [30]. Conversely, drugs that increase 2-AG and/or AEA levels induce antidepressant-like effects in animal models [34]. Overall, these studies suggest that the ECS plays a central role in MDD neurobiology and in the antidepressant effect [35]. Given the critical role of the ECS in regulating neurotransmitter systems involved in MDD neurobiology, such as glutamate, GABA and serotonin [36], as well as their prominent role in synaptic plasticity [37], we hypothesized that the ECS may be involved in the rapid antidepressant effect of KET.

Recent evidence indicates that striatal 2-AG and CB1activation are involved in the psychostimulant effect of KET in unstressed mice [38]. Accordingly, our group reported that the psychostimulant effect of KET is reduced in mice with impaired CB1 signaling, but not its behavioral effect in the forced swim test [39]. However, this study used only naïve animals, thus limiting the translational interpretation of the findings [40].

To overcome this knowledge gap and clarify the involvement of the ECS in KET's fast antidepressant effects, we used rats presenting depressive phenotype alongside dysfunctions in the cortical ECS: the Flinders Sensitive rat Line (FSL) [41]. These animals constitute a well validated model of depression based on selective breeding [42]. When compared with their controls, the Flinders Resistant Line (FRL), the FSL presents abnormal endocrine and emotional responses to stress (e.g. increased learned immobility in the Forced Swimming Test - FST), and impaired synaptic plasticity in limbic regions, all common features observed in depression [43]. The model also presents good predictive validity, since their molecular and behavioral phenotype is reversed by chronic treatment with monoaminergic antidepressants or by acute KET administration [42,44]. Moreover, their selective breeding, initially based on the sensibility to anticholinesterase drugs, is consistent with observations that the muscarinic acetylcholine antagonists induce rapid antidepressant effects [45,46], making these animals ideal for studying neurobiological questions [44].

A previous study from our group first described that FSL animals have reduced levels of 2-AG in the prefrontal cortex (PFC), when compared to FRL [28], indicating that a dysregulation in the cortical ECS could subside the increased vulnerability of FSL to stress. However, the previous study used only naïve animals, and it did not investigate if antidepressants could reverse the 2-AG deficits in the PFC. Furthermore, there is no study reporting if the rapid antidepressant effect of KET involves the regulation of the ECS in the PFC. Therefore, FSL stands out as the ideal model to investigate that question.

Herein, we investigated the participation of the cortical endocannabinoid system in the antidepressant effect induced by the (S)-ketamine (S-KET), which is the enantiomer approved for clinical use in depressed patients [47,48]. We used an integrative approach that combined behavioral evaluations, molecular biology and lipidomic analyses, as well as computational predictions of the binding affinity and binding mode of KET and its enantiomers to different targets of the ECS. Taken together, our results shed light on the possible involvement of the ECS in S-KET antidepressant properties. Since S-KET use is limited due to considerable side-effects (e.g. increased risk of abuse, psychotomimetic effects and dependence) and concerns about its safety and efficacy [49,50], our data can offer new perspectives for achieving rapid antidepressant effects by targeting the ECS.

2. Material and methods

2.1. Animals

Male FSL and their control counterpart FRL (200–390 g, 8–11 weeks old) were obtained from breeding colonies kept at the Translational Neuropsychiatry Unit (Aarhus University Hospital, Denmark). All rats were housed in pairs within standard cages (425 × 266 × 185 mm), under conditions of 22 ± 2 °C temperature, 60 ± 5 % relative humidity with *ad libitum* access to food and tap water. The rats were kept on a 12-hour-light/-dark cycle (lights on at 6 a.m) and the experiments were performed in the light period. Enrichment items, such as a stainless-steel tunnel shelter, nesting material, and a wooden stick were available to the rats throughout the study period. The experimental procedures received approval from the Danish National Committee for Ethics in Animal Experimentation (Protocol number: 2021–15–0201–01010) and were conducted in accordance with the guidelines of the European Community Council Directive 2010/63/EU.

2.2. Drugs

S-ketamine hydrochloride (15 mg/kg; Pfizer, Ballerup, Denmark, hereafter referred to as S-KET) was diluted in sterile saline (Sal) [51]. Rimonabant hydrochloride (RIMO) (1 mg/kg; Sigma-Aldrich, St. Louis, MO, USA) was dissolved in cremophor–ethanol–saline (1:1:18, v/v) [39]. All drugs were freshly prepared before the experiment, and injections were given intraperitoneally (i.p.) in a volume of 1 mL/kg.

2.3. Behavioral tests

The animals were brought from the breeding stable to the

experimental rooms and allowed to habituate in their home-cage for at least one hour before the start of the behavioral testing. The FSL animals were randomly assigned to the different treatments, which were randomly distributed along the experimental session (from 8 am to 12 pm) to avoid circadian influences in the results.

As the experiments were run according to the availability of FSL and FRL from the stable, the sample size in the groups is not the same between experimental conditions. However, the sample size is in line with previous studies which detected significant differences between FRL and FLS (control vs ketamine) [51,52]. The open field test (OFT) and the forced swim test (FST) were used to detect phenotypic differences between FSL and FRL rats, as well as treatment effects, considering that previous works demonstrated that the acute treatment with S-KET induces significant behavioral and molecular effects in FSL that are consistent with its antidepressant action [52,53]

2.3.1. Open field test (OFT)

The animals were placed within a 1-square meter arena, where the light intensity at the center was maintained at 25–30 lux, and at the periphery, it ranged between 10 and 20 lux. During this time, their behavior was actively monitored for 10 min, and the total distance travelled (meter; m) was measured using EthoVision® XT16 (Noldus Information Technology, Wageningen, Netherlands) [54] (Fig. 1A). Immediately after, the animals were transported to a neighboring room where they were exposed to the forced swim test.

2.3.2. Forced Swim test

We used a well-validated protocol for FSL, as previously described [43]. Briefly, each rat was placed in a cylinder (24 cm diameter and 60 cm height) filled with tap water maintained at 24 ± 1°C, with the water reaching 40 cm in height. To eliminate olfactory cues, the water was changed between each session. The session (7 minutes) was recorded on video and subsequently, the behaviors of immobility, swimming, and struggling were manually evaluated during the first 5 minutes at 5-second intervals by a blinded experimenter [55] (Fig. 1A). The animals were not pre-exposed to a swim session because FSL present increased vulnerability to stress, displaying higher immobility in the FST without pre-exposure to a swim session [53,56].

2.4. Experimental design

- Experiment 1: to investigate if S-KET would modulate the ECS in animals that present depressive-like behavior, FSL rats received one intraperitoneal injection of saline (Sal, 1 mL/Kg) or S-KET (15 mg/kg), 1 h before the behavioral tests. FRL rats received only saline and were used as strain controls to unravel differences in the ECS associated with stress vulnerability in the FSL. Since FRL animals are naturally resilient to stress and present low immobility in the FST, even in the absence of antidepressant treatment [43], this study used only 3 experimental groups (FRL-Sal, FSL-Sal and FSL-CBD) to avoid unnecessary use of animals and comply with the 3 R principles in animal experimentation (https://nc3rs.org.uk/who-we-are/3rs). All 3 groups were run in parallel and, 1 h after the last injection, the rats were individually placed in the OFT for 10 min and then in the FST for 7 minutes, considering strain and treatment randomization.

- Experiment 2: to evaluate the participation of CB1 receptors in S-KET effects, FSL animals received a first injection (i.p) of vehicle (Veh: cremophor-ethanol-saline) or RIMO and, 30 min later, they received a second injection (i.p) of Saline or S-KET. One hour after the second injection, the animals were subjected to the behavioral tests described above. In this experiment, the animals treated with vehicle followed by S-KET were subdivided into two groups according to their immobility time - low immobility (LI; responder) and high immobility (HI; non-responder)- due to the high response variability between animals in this. Those animals displaying immobility time below 20 % of the average of FSL control group were classified as LI, while those above this value were considered HI [57].

2.5. Molecular analysis

2.5.1. Sample collection and preparation

Immediately after the FST, the animals were taken to a separate room and euthanized by decapitation. The PFC was rapidly dissected on powdered dry ice, carefully divided into left and right hemispheres, and stored at −80 °C until further analysis. The hemispheres of the PFC were randomized and half of them were targeted for lipidomic analysis, and the other half were processed for RNA extraction and protein isolation using PARIS™ kit (Thermo Fisher Scientific, USA), following the manufacturer's instructions.

2.5.2. Real Time quantitative PCR (RT-qPCR)

The RNA was quantified and then converted to cDNA using iScript cDNA Synthesis Kit (Bio-Rad). RT-qPCR was performed with iTaq Universal Probes Supermix (Bio-Rad) using a MX3005 qPCR system (Agilent Technologies, Glostrup, Denmark). The gene expression of *Cnr1*, *Cnr2*, *Gpr55*, *Faah*, *Mgll* and Transient receptor potential vanilloid 1 (*Trpv1*) was determined relative to the housekeeping, Hprt, and the fold change was calculated using the $2^{-\Delta\Delta CT}$ threshold cycle method [58] (Supplementary Table S1).

2.5.3. Western blot analysis

Total protein concentration was assessed using the Pierce BCA Protein Kit (Thermo Scientific) according to the manufacturer's guidelines. The samples were subsequently applied for dual fluorescence western blot analysis [59]. Briefly, 12 µL of each aliquot containing 24 µg of total protein were loaded into an SDS-polyacrylamide gel (26 wells – NuPAGE 10 % Bis-Tris Midi Gel – Thermo Scientific). The separated proteins were transferred to a 0.2 µM nitrocellulose membrane (Midi format, Bio-Rad) using the Bio-Rad Trans-Blot Turbo Transfer System. The membrane was blocked in interception blocking buffer (IBB; Licor) for one hour at room temperature and then incubated with primary antibody diluted in IBB/0.1 % Tween-20 at 4 °C overnight: mouse anti-β-actin (1:2000; Licor 926–42212), rabbit anti-β-actin (1:2000; Licor 926-42210), rabbit anti-CB1 (1:1000; Abcam ab2703), mouse anti-CB2 (1:500, Santa Cruz sc-293188), mouse anti-FAAH (1:500, Sigma WH0002166M7). On the next day, the membranes were washed in TBS+ 0.1 % Tween-20 (4 time for 5 min) and incubated with secondary antibody diluted in IBB solution with TBS + 0.1 % Tween-20 at room temperature for 1 h protected from light: Goat anti-rabbit 800CW, Goat anti-mouse 800CW, Goat anti-mouse 680RD and Goat anti-rabbit 680RD (1:10000; Licor). The membranes were washed four times in TBS with 0.1 % Tween-20 and once with TBS buffer for 5 min. The protein levels were assessed using Odyssey CLx Scan (Licor) and the results were expressed as percentage of control group (FRL-Sal).

2.5.4. Lipidomic analysis – ECS levels

The levels of endocannabinoids, including 2-AG, AEA, Palmitoyl-Ethanolamide (PEA), Docosahexaenoyl-Ethanolamide (DHA-EA), Oleoyl-Ethanolamide (Oleoyl-EA), Linoleoyl-Ethanolamide (Linoleoyl-EA), and Eicosapentaenoyl-Ethanolamide (EPA-EA) were assessed in the PFC samples using LC/ESI-MS/MS lipidomic technology [57,60]. For sample preparation, aproximately 20 mg of tissue was homogenized in citric acid buffer, and then an internal standard was added. The sample was extracted twice using ethyl acetate. The combined organic layer was evaporated on a heating block at 40 °C under a stream of nitrogen. The solid residue was resolved in 100 µL 60 % methanol in water. The prepared samples were analyzed using an Agilent 1290 HPLC system with a binary pump, an autosampler, and a column thermostat with an Agilent Poroshell C18 column. The HPLC was coupled with an Agilent 6495 Triple Quad mass spectrometer with an electrospray ionization source. Analysis of ECS was performed with the Multiple Reaction Monitoring in positive mode. Data analysis and quantification were performed with

Agilent Mass Hunter Software using individual calibration curves for each compound (Lipidomix GmbH). The results were expressed as ng/g of tissue.

2.5.5. S-KET effects on CB1 receptor binding

Real-time autoradiography was performed to evaluate the specific binding of a radiolabeled CB1 antagonist, [^{3}H]SR141716A, to CB1 receptors in brain slices of FRL-Sal and FSL (Sal and S-KET) containing the PFC, as previously described [61]. Briefly, each slide contained 4–6 sequential brain slices, with an additional adjacent slide used to determine non-specific binding. The selection of slides at the PFC level followed the coordinates outlined in the Paxinos and Watson stereotaxic rat brain atlas. The slides were pre-incubated for 20 min in a 50 mM Tris-HCL buffer (pH 7.4), and then incubated for 90 min in the same buffer containing 0.5 % albumin and 0.5 nM [3 H]SR141716A [Specific Activity 1883 GBq/mmol (50.9 Ci/mmol); PerkinElmer]. For the non-specific binding assay, adjacent sections were incubated in the same solution as used for total binding but supplemented with 3 μM AM251, a CB1 receptor antagonist, diluted in DMSO (Tocris Bioscience – #1117). Specific binding was determined by subtracting non-specific binding (cp/min/mm^2) from total binding (cp/min/mm^2). All autoradiography acquisitions were conducted for 12 hours using a BeaQuant autoradiography system (ai4r, France). For the analysis, PFC-specific areas were manually drawn in Beamage software (version 3.5.2) (ai4r, Nantes, France). The results were expressed as a percentage of the control group (FRL-Sal).

2.6. Data analysis

The mean values of individual behavioral and molecular data were compared between the rat strains (FRL and FSL) and between FSL groups treated with Saline (Sal) and S-KET using Student's *t*-test. If the variances between groups were not homogenous, the Mann–Whitney test was used instead. One-way ANOVA, followed by Tukey's post hoc test was applied in the experiment using RIMO.

To evaluate possible correlations between the behavioral changes and each endocannabinoid, regardless of strain or treatment effects, we ran a correlation matrix (two-tailed) with pooled results of all 3 experimental groups. To assess treatment effects in the overall endocannabinoid activity, we created a composite z-score based on the z-score of multiple endocannabinoids and immobility time. This approach allowed us to integrate the effects of various components into one standardized metric (endocannabinoid index), making it easier to compare the overall endocannabinoid tone between different treatment groups.

The endocannabinoid index was calculated by averaging the z-scores of various endocannabinoids (1-AG, 2-AG, 2-AG SUM, AEA, PEA, DHA-EA, Oleoyl-EA, Linoleoyl-EA, and EPA-EA). Each z-score derived from the formula (FSL data − mean of FRL group)/standard deviation of FRL group). The overall endocannabinoid index is then expressed as:

Endocannabinoid index $= 1/n\sum_{i=1}^{n} Zi$, where Z_i represents the z-score of each individual component, and n is the total number of components included in the index.

Finally, to evaluate if behavioral changes in the FST would reflect changes in the endocannabinoid index, we performed a linear regression analysis between the normalized immobility time ((FSL − mean of FRL group)/standard deviation of FRL group)) and the endocannabinoid index. Results were considered statistically significant when $p < 0.05$. All analyses were performed using GraphPad Prism 9.0.

Significant outliers were removed from the statistical analysis through GraphPad' Outlier calculator (Grubbs; Alpha = 0.05) but kept in the figure in a highlighted way for transparency of the results. The sample size for each experiment was determined based on the availability of rats, which are bred in our animal facility, but are sufficient to detect differences between groups, based on previous reports [51,52].

2.7. Computational methods

2.7.1. 3D protein structures

The 3D structures of human CB1, CB2, MAGL and Fatty Acid Binding Protein 5 (FABP5) were based on experimental structures available at the protein data bank (PDB) [62,63] IDs 5XRA [64], 6KPF [65], 5HZ5 [66] and 5ZUN [67], respectively. The X-ray structure of CB1 complexed to the respective selective agonist AM11542 (EC_{50} = 3.5 nM) showed a resolution of 2.8 Å. The Cryo-EM structure of CB2 complexed to the respective selective agonist AM12033 (EC_{50} = 0.37 nM) presented a resolution of 2.9 Å. The X-ray structure of MAGL complexed to the noncovalent inhibitor 1-(2′-Chlorobiphenyl-3-yl)-4-[4-(1,3-thiazol-2-ylcarbonyl)piperazin-1-yl]pyrrolidin-2-one (named 3 l) (IC_{50} = 0.64 nM) presented resolution of 1.35 Å. The X-ray structure of FABP5 complexed with the selective inhibitor 6-Chloro-4-phenyl-2-piperidin-1-yl-3-(1H-tetrazol-5-yl)-quinoline (IC_{50} = 3.6 nM) presented a resolution of 1.4 Å. The modelled 3D structures of human FAAH, GPR55 and TRPV1 were obtained from the Alphafold protein structure database [68] (Uniprot IDs O00519, Q9Y2T6 and Q8NER1, respectively). The GPR55 presented a high model confidence with an average per-residue model confidence score or (Local Distance Difference Test) pLDDT of 87.1; FAAH presented a very high model confidence with an average pLDDT of 95.37 and TRPV1 presented a high model confidence with an average pLDDT of 71.85. For TRPV1, we also build the homo-4-mer using the GalaxyHomomer [69,70] web tool, to mimic the tetrameric spatial conformation of this channel in the plasmatic cell membranes.

2.7.2. Protein and ligand preparation

The protein structures were prepared using the Protein Preparation Wizard tool from Maestro molecular modelling suite from Schrödinger©, USA [71]. Briefly, hydrogen atoms were added, and the overall structure energy was minimized using the OPLS-2005 force field [72]. The ligands were prepared through the LigPrep tool also from Maestro suite, correcting protonation, according to Epik, and performing energy minimization under OPLS-2005 force field [73,74]. The grid box was prepared using the Receptor Grid Generation tool, and the grids were on the residues close to co-crystallized ligand or on the predicted binding site, with grid boxes of dimensions 20 × 20 x 20 Å. The protein binding sites of CB1, CB2, FABP5 and MAGL were based on their co-crystalized ligands. The binding site of FAAH was based on the crystal structure of the homologous fatty acid amide hydrolase (PDB 2VYA) [75] from *Rattus norvegicus*, complexed with the selective inhibitor PF-750. The TRPV1 binding site was based on electron microscopy structure of TRPV1 from *Rattus norvegicus* (PDB 5IRX) [76] in complex with vanilloid receptor agonist Tau-theraphotoxin-Hs1a (referred as DkTx). Considering the absence of available highly homologous structures of the G-protein receptor GPR55 with co-crystalized ligands, the binding site of this target was predicted using FTsite server as established previously [77].

2.7.3. In silico calculations and data presentation

The molecular dockings calculations were performed through Glide software from Maestro suite, Schrödinger© [78–80], in the standard-precision (SP) mode, considering the ligand fully flexible and the protein rigid [71]. The resulting ligand-protein complex structures were uploaded in the open-source web tool protein-ligand interaction profiler (PLIP) for automated detection and visualization of relevant non-covalent protein-ligand contacts in uploaded 3D ligand-protein structures [81]. Moreover, Visual Molecular Dynamics (VMD) [82] and Pymol programs were used for the visual inspection of the docking poses and to render the 3D images of the ligand-protein complexes.

3. Results

3.1. Acute treatment with S-KET induces antidepressant-like effect in FSL rats

As expected, FSL injected with saline exhibited significantly higher immobility time compared to FRL under the same conditions (Student's *t*-test: t(10) = 5.624). Administration of S-KET reduced immobility in FSL animals (Student's *t*-test: t(14) = 4.953; $p < 0.05$; Fig. 1B). Saline-injected FSL displayed significantly less swimming time than FRL (Student's *t*-test: t(10) = 8.256) and S-KET increased swimming time in FSL (Student's *t*-test: t(14) = 2.284; $p < 0.05$; Fig. 1C). There were no observable differences in struggling time between saline-treated FSL and FRL (Student's *t*-test: t(10) = 0.5698). Nevertheless, S-KET increased struggling time in FSL (Student's *t*-test: t(14) = 3.712; $p < 0.05$; Fig. 1D). No significant alterations were noted in locomotor activity (Student's *t*-test: t(10) = 0.07008 and t(14) = 1.486; $p > 0.05$; Fig. 1E). These results support previous findings describing the acute antidepressant-like effect of S-KET in FSL animals [55].

3.2. S-KET effects in the gene expression and protein levels of components of the ECS in the PFC

To investigate if the antidepressant-like effects of S-KET could be associated with rapid changes in the expression of genes coding for proteins of the ECS, we evaluated the transcript levels of the main receptors involved in endocannabinoid signaling, CB1, CB2, GPR55 and TRPV1. No significant differences were detected in the transcript levels of receptors between FSL and FRL animals, although a tendency towards increased GPR55 gene expression was detected in FSL animals (Mann-Whitney test: U= 5; p = 0.07; Fig. 2C). S-KET significantly decreased the gene expression of CB1 (Student's *t*-test: t(14) = 2.146; $p < 0.05$; Fig. 2A), but did not affect the gene expression of other receptors investigated (CB2: Mann-Whitney test: U= 24,5; GPR55: Mann-Whitney test: U=14; TRPV1: t(14) = 1.533; $p > 0.05$; Fig. 2B-D). The enzymes FAAH and MAGL, responsible for synthesizing the main endocannabinoids AEA and 2-AG, were also evaluated. FAAH gene expression was increased in FSL animals (Student's *t*-test: t(10) = 2.234; $p < 0.05$; Fig. 2E), which was attenuated by S-KET (Student's *t*-test: t(14) = 2.062; p = 0.058; Fig. 2E). No differences were observed between the strains or treatments for MAGL transcripts (Student's *t*-test: t(9) = 0.432; t(13) = 0.087; $p > 0.05$; Fig. 2F).

We subsequently assessed protein levels of CB1, CB2 and FAHH, based on their relevance for endocannabinoid signaling, and on the gene expression changes (Fig. 2). The western blot data demonstrated that there was no significant difference in CB1 and CB2 levels in the PFC of FSL and FRL animals (CB1: Mann-Whitney test: U=18; CB2: Student's *t*-test: t(10) = 0.0057; $p > 0.05$) and no effect of S-KET treatment either (CB1: Student's *t*-test: t(14) = 0.1176; CB2: Student's *t*-test: t(14) = 0.1571; $p > 0.05$; Fig. 3A-B). Similarly, no difference was observed between the strains (Student's *t*-test: t(10) = 0.5360; $p > 0.05$) and treatments in FAAH levels (Student's *t*-test: t(14) = 1.216; $p > 0.05$; Fig. 3C).

3.3. S-KET increases specific binding to CB1 receptors in the PFC of FSL

There were no differences between FSL and FRL animals in the binding of [^{3}H]SR141716A to CB1 receptors (Mann-Whitney test: U=18; $p > 0.05$). However, S-KET increased the specific binding of [^{3}H]SR141716A to CB1 in FSL by 15.78 % compared to FSL-Sal (Student's *t*-test: t(11) = 2.124; p = 0.057; Fig. 3D).

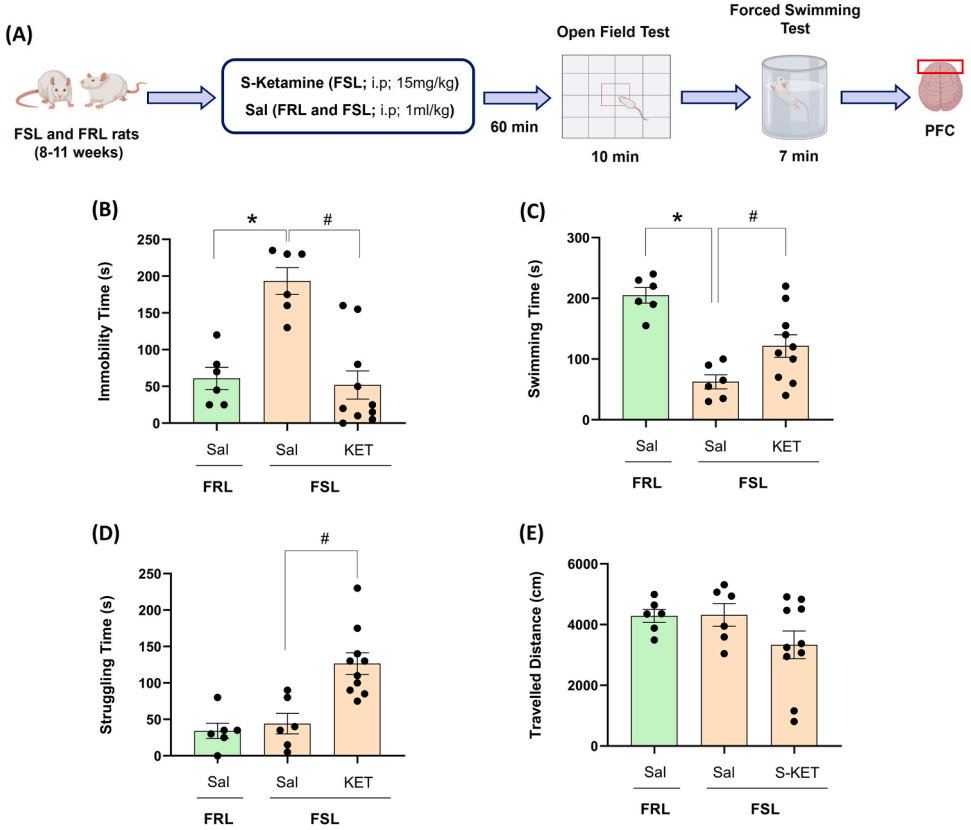

Fig. 1. Effect of the acute treatment with S-KET in FSL rats in the FST and OFT. (A) Schematic diagram of experimental design. (B) Immobility time; (C) swimming time; (D) struggling time in FST, and (E) travelled distance in OFT. Data represent the mean ± SEM. *p < 0.05 from FRL Veh group, #p < 0.05 from FSL Veh group (Student's *t*-test); n = 6–10/group.

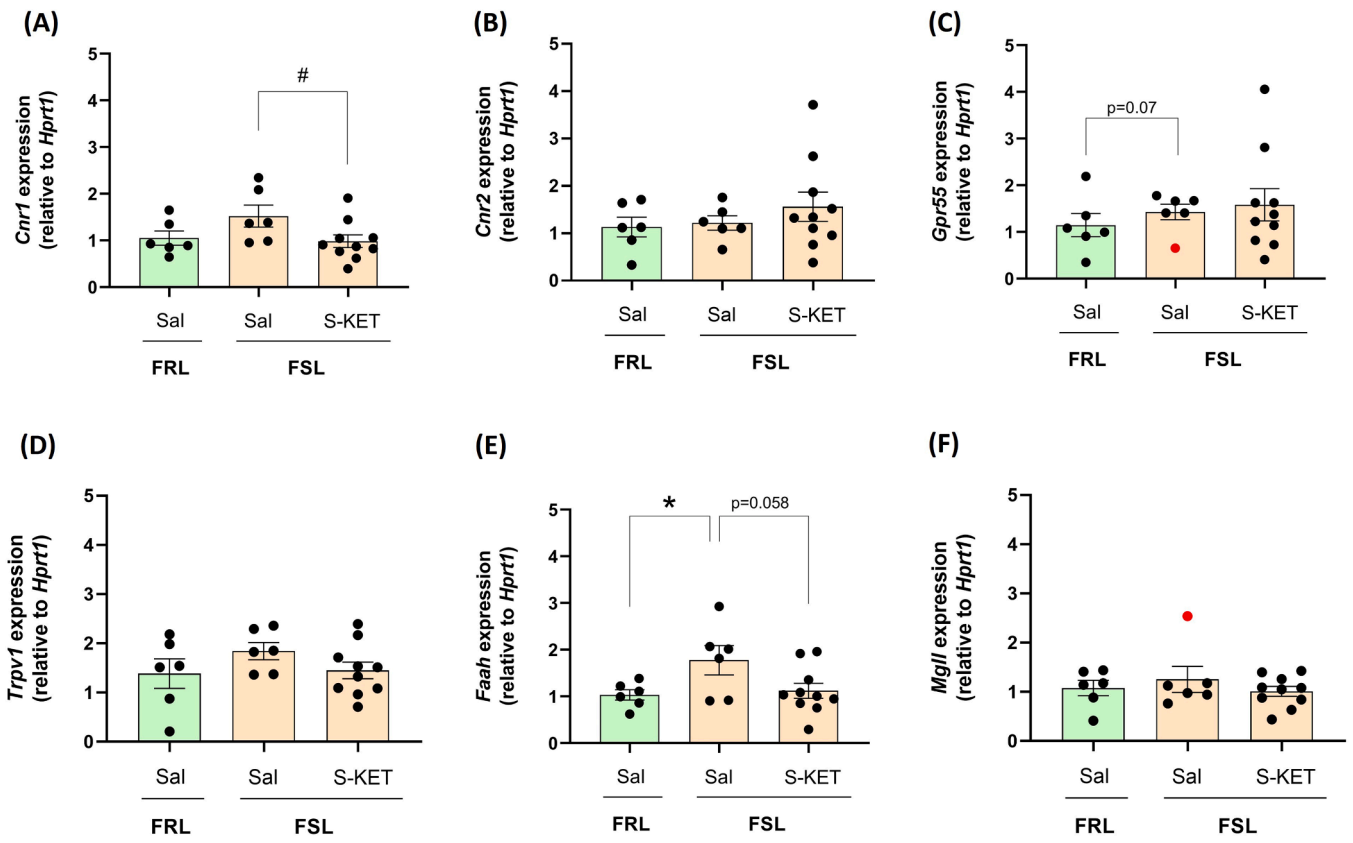

Fig. 2. Effect of the acute treatment with S-KET on the expression of candidate genes in the PFC of Flinders rats. Gene expression levels of (A) CB1 (*Cnr1*); (B) CB2 (*Cnr2*); (C) GPR55 (*Gpr55*); (D) TRPV1 (*Trpv1*); (E) FAAH (*Faah*) and (F) MAGL (*Mgll*) relative to *Hprt1*. Data represent the mean ± SEM. *p < 0.05 from FRL Veh group, #p < 0.05 from FSL Veh group (Student's *t*-test and Mann-Whitney test); n = 5–10/group. Significant outliers were removed from the statistical analysis and are represented by red dots.

3.4. S-KET effects on endocannabinoid levels in the PFC

In addition to investigating the effects of S-KET on the main targets of the ECS, we also evaluated how it regulates endocannabinoid levels in the PFC. The lipidomic analysis demonstrated that 2-AG+ 1-AG levels (2-AG SUM) are decreased in the PFC of FSL-Sal compared to FRL-Sal (Student's *t*-test: t(10) = 4.194; p < 0.05), in agreement with our previous publication using naive animals [28]. Treatment with S-KET induced a trend in restoring the levels of 2-AG SUM in FSL animals (Student's *t*-test: t(14) = 1.876; p = 0.08; Fig. 4A). Similar results were observed for isolated 2-AG levels (FSL vs FRL: Student's *t*-test: t(10) = 1.932; p = 0.082; FSL-S-KET vs FLS-Sal: Student's *t*-test: t(14) = 1.979; p = 0.067; Supplementary Figure S1B). No differences were observed in 1-AG levels between the strains (FSL vs FRL: Student's *t*-test: t(10) = 0.2778; FSL-S-KET vs FSL-Sal: Student's *t*-test: t(14) = 0.7712; p > 0.05; Supplementary Figure S1A).

A tendency towards decreased PEA levels was observed in FSL animals (Student's *t*-test: t(10) = 2.187; p = 0.053) which remained unaffected by S-KET (Student's *t*-test: t(14) = 0.1087; p > 0.05; Fig. 4C). Linoleyl-EA was slightly increased in FSL animals (Mann-Whitney test: U= 7; p = 0.093), which was attenuated by S-KET (Mann-Whitney test: U=12; p = 0.087; Fig. 4F). There was no difference in AEA, DHA-EA, Oleoyl-EA, and EPA-EA levels between strains (AEA: Student's *t*-test: t(10) = 0.2167; DHA-EA: Student's *t*-test: t(10) = 0.2240; Oleoyl-EA: Student's *t*-test: t(10) = 0.0672; EPA-EA: Student's *t*-test: t(10) = 0.5423; p > 0.05) or treatment (AEA: Student's *t*-test: t(14) = 0.2427; DHA-EA: Student's *t*-test: t(14) = 0.5813; Oleoyl-EA: Student's *t*-test: t(14) = 0.4323; EPA-EA: Student's *t*-test: t(14) = 0.7174; p > 0.05; Fig. 4B, D and E and Supplementary S1C).

To identify possible associations between behavioral changes and specific endocannabinoids, regardless of the strain or treatment, we performed a correlation analysis[83]. As expected, the specific correlation analysis showed a negative association between immobility and active behaviors: swimming (*r*: −0.703; p < 0.05) and struggling (*r*: −0.526; p < 0.05). Immobility also significantly correlated with 2-AG SUM (*r*: −0.291; p < 0.05) and with Linoleyl-EA levels (*r*: 0.425; p < 0.05). Moreover, swimming was positively correlated with 2-AG SUM (*r*: 0.532; p < 0.05) and PEA levels (*r*: 0.456; p < 0.05). No significant correlation was observed between endocannabinoid levels and struggling behavior (Fig. 5A and Supplementary Table S2).

To evaluate if such correlations derived primarily from treatment or strain effects, we performed new correlation analysis considering each group separately (FSL-Sal and FSL-S-KET). In FSL-S-KET groups, the higher the immobility, the lower the levels of AEA (*r*: −0.775; p < 0.05), PEA (*r*: −0.774; p < 0.05), DHA-EA (*r*: −0.715; p < 0.05) and Oleoyl-EA (*r*: −0.727; p < 0.05)(Fig. 5C and Supplementary Table S2). Interestingly, the linear regression analysis evaluating S-KET effects in the endocannabinoid index showed that the changes in the immobility were significantly correlated with changes in the endocannabinoid tone (R^2=0.84, p < 0.05) (Fig. 5D).

3.5. S-KET effects upon administration of Rimonabant

Since S-KET affected CB1 availability (Fig. 3D) and endocannabinoid levels (Fig. 4), we evaluated if pre-treatment with RIMO, a CB1 antagonist/inverse agonist [84], could interfere with S-KET-induced behavioral effects. One-way ANOVA revealed a significant difference between treatments ($F_{2,17}$=8.365, p < 0.0015), but without significant differences between S-KET and vehicle group (p > 0.05, Tukey). However, a significant effect was observed when S-KET was co-administered with

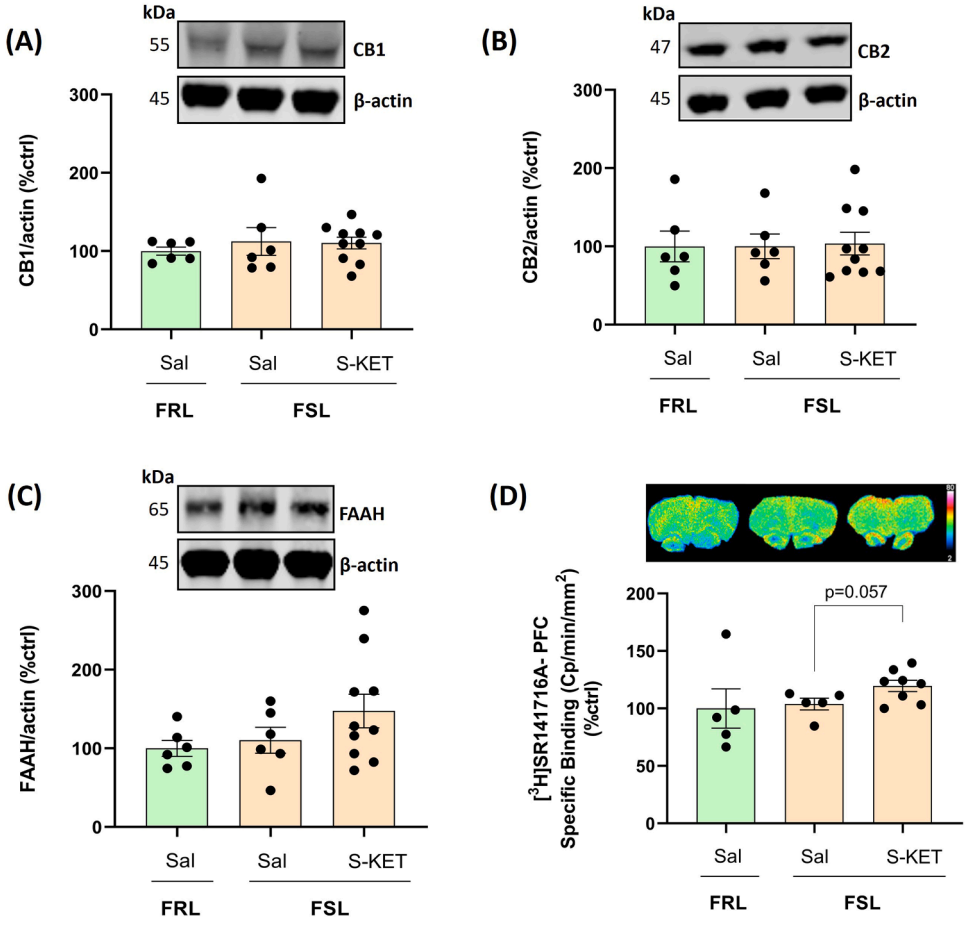

Fig. 3. Effect of the acute treatment with S-KET on the protein levels and specific binding to CB1 receptors in PFC of Flinders rats. Representative Western Blotting bands and bar graphs of the individual proteins normalized by β-actin and represented by % of control (FRL Veh) of (A) CB1; (B) CB2; and (C) FAAH. (D) Representative autoradiograms and quantification of the specific binding of the CB1 receptor antagonist, [^{3}H]SR141716A, to CB1 receptors represented by % of control (FRL Veh). Data represent the mean ± SEM. (Student's *t*-test and Mann-Whitney test); n = 5–10/group.

RIMO ($p < 0.05$, Tukey; Supplementary Figure S1D). To avoid confounding factors due to the lack of a robust effect of S-KET, we further analyzed the data dividing the animals into responders and non-responders. The same results were observed for the animals treated with RIMO followed by S-KET ($F_{3,16} = 12.49$; $p < 0.05$; One-way ANOVA followed by Tukey's test; Fig. 6B). There was no difference between the immobility time of animals that responded to S-KET (Veh-LI + S-KET) and those previously treated with rimonabant (RIMO + S-KET) ($F_{3,16} = 12.49$; $p > 0.05$; One-way ANOVA followed by Tukey's test; Fig. 6B). There was also no difference in the travelled distance ($F_{3,16} = 2.372$; $p > 0.05$; One-way ANOVA followed by Tukey's test; Fig. 6C).

3.6. *In silico calculations of S-KET effects on molecules of the ECS*

Considering that S-KET upregulated endocannabinoids and CB1 binding in FSL animals, but its behavioral effects were not blocked by RIMO, we explored the possibility that S-KET could target other components of the ECS. To investigate the binding affinity, ligand efficiency and molecular interactions performed by S-KET and its metabolites in different targets of the ECS, we performed docking calculations of S-KET, S-norketamine (S-NORK) and (2S,6S)-hydroxynorketamine ((2S,6S)-HNK) against CB1, CB2, MAGL, FAAH, GPR55, TRPV1 and FABP5 (see Table 1 and Supplementary Table S3). As a comparison, the known ligands of each target were also submitted to docking calculations. Docking score predicts the binding affinity of a compound in the target binding site, while ligand efficiency (LE)[85,86] normalizes the binding affinity with respect to number of heavy atoms (n). The more negative a docking score, the more favorable the ligand-protein binding interaction. LE = (ΔG)/n. LE value for oral drugs or hits ≥ 0.3 Kcal mol^{-1}·non-hydrogen atom^{-1} indicates a satisfactory result [86]

The best docking score and LE results for S-KET were observed for FAAH, CB1, CB2 and GPR55 targets (Table 1). For all these targets, S-KET binds efficiently, exhibiting favorable LE values ≥ 0.3 Kcal mol^{-1}·non-hydrogen atom^{-1}. While for the (2S,6S)-HNK metabolite, the FAAH, CB2, MAGL and GPR55 targets presented the best docking scores and LE results (Supplementary Table S3). For S-NORK, the FAAH, CBR2 and GPR55 targets showed the best results (Supplementary Table S3). The FAAH, CB2 and GPR55 targets presented satisfactory binding affinity predictions for both S-KET and metabolites. In Fig. 7, we show the predicted binding mode of S-KET against the targets CB1 (A), CB2 (B), GPR55 (C), FAAH (D), MAGL (E) and FABP5 (F), highlighting the main interactions with the binding site residues. The predicted binding modes for (2S,6S)-HNK and S-NORK are presented in Supplementary Figures S2 and S3.

In docking calculations, S-KET interacts with FAAH residues through hydrogen bond interactions with Gln273 and Cys269 and through hydrophobic interactions with Met191, Phe192, Ile 238, Val270 and Phe388 (Fig. 7A), presenting a docking score of −8.17 Kcal mol^{-1} and ligand efficiency of 0.51 Kcal mol^{-1}·non-hydrogen atom^{-1} (Table 1). Similarly, we performed docking calculations for a non-covalent inhibitor 8 (1-{(3S)-1-[4-(1-benzofuran-2-yl)pyrimidin-2-yl]piperidin-3-yl}-3-ethyl-1,3-dihydro-2H-benzimidazol-2-one) ($IC_{50} = 10$ nM) to allow a comparison with S-KET and its metabolites, it showed a docking score of −9.75 Kcal mol-1 and ligand efficiency of 0.37 Kcal mol-1·non-hydrogen

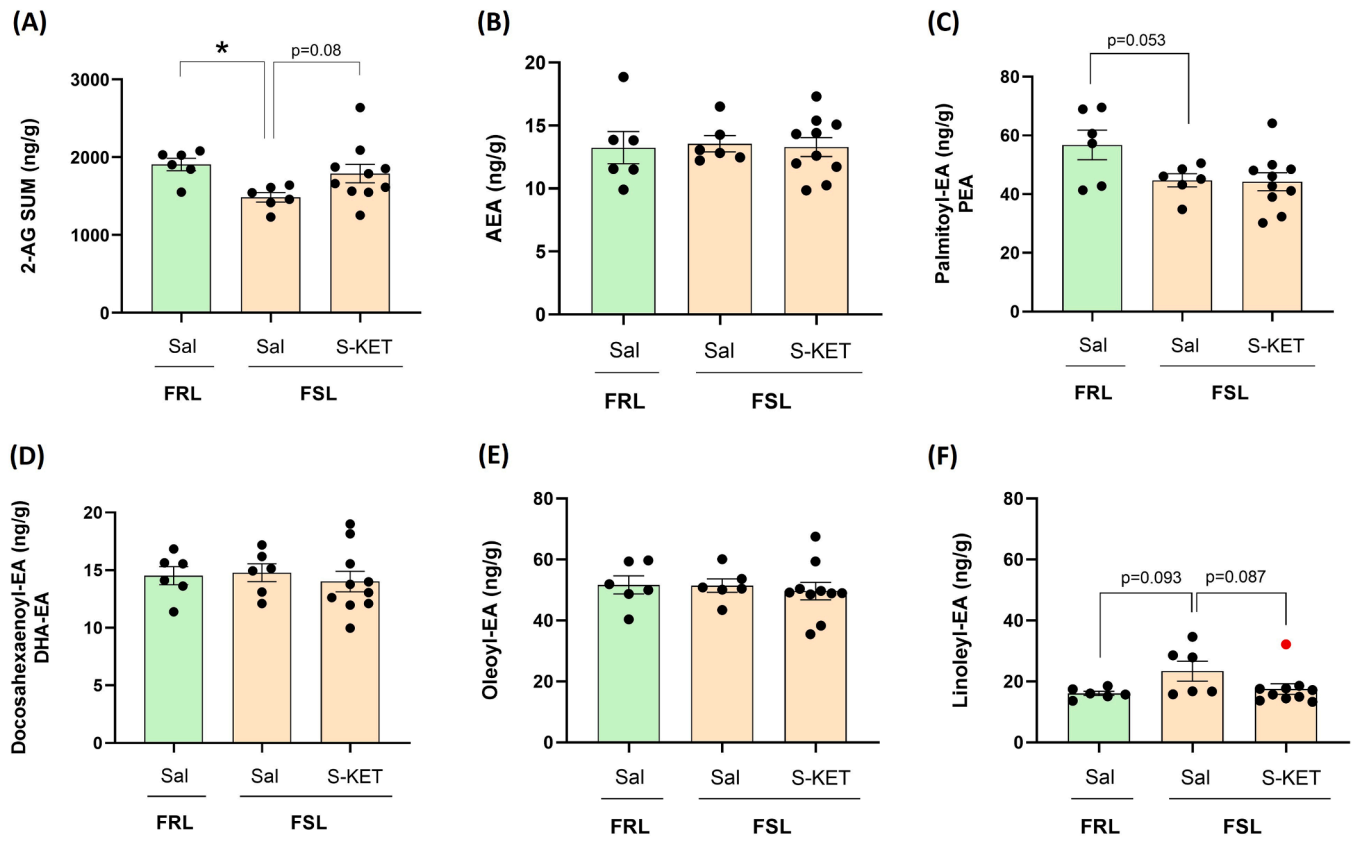

Fig. 4. Effect of the acute treatment with S-KET on ECs levels in PFC of Flinders rats. Levels of (A) 2-AG SUM; (B) AEA; (C) Palmitoyl-EA – PEA; (D) Docosahexaenoyl-EA – DHA-EA; (E) Oleoyl-EA and (F) Linoleoyl-EA represented by ng/g of PFC tissue. Data represent the mean ± SEM. *p < 0.05 from FRL Veh group (Student's *t*-test and Mann-Whitney test); n = 6–9/group. Significant outliers were removed from the statistical analysis and are represented by red dots.

atom-1. This known ligand (inhibitor 8) presented π-stacking interactions with Trp531 and hydrophobic interactions with Ile238, Phe381 and Thr488 residues. S-KET and the non-covalent inhibitor 8 presented some similar interactions on the FAAH binding site.

The molecular docking of S-KET with the CB1 binding site suggests that S-KET interacts through π-stacking interactions with Phe174 and His178 residues; as well as hydrophobic interactions with Phe170, Leu193, Val196, Phe268 and Phe379 (Fig. 7B), resulting in a docking score of −7.62 Kcal mol^{-1} and ligand efficiency of 0.47 Kcal mol^{-1}·non-hydrogen $atom^{-1}$. Comparatively, the selective CB1 agonist AM11542 which is the co-crystalized ligand of CB1 receptor (PDB ID 5XRA) mainly performs hydrophobic and aromatic interactions with residues from extracellular loop 2 (ECL2), helices III, V, VI and VII. The tricyclic tetrahydrocannabinol ring system of AM11542 made π-stacking interactions with Phe268 (ECL2), Phe177, Phe189 and Phe379 residues, and the phenolic hydroxyl made hydrogen bond with Ser383 [87] residue. The redocking result for AM11542 presented a docking score of −11.8 Kcal mol^{-1}, ligand efficiency of 0.42 Kcal mol^{-1}·non-hydrogen $atom^{-1}$ ligand efficiency of 0.42 Kcal mol-1·non-hydrogen atom-1 and root mean square deviation (RMSD) of 0.58 Å, indicating that our docking protocol was able to reproduce the experimental binding mode of AM11542 in CB1.

S-KET interacts with CB2 through a hydrogen bond with Thr114 and hydrophobic interactions with Phe87, Ile110, Phe183, Leu191, Trp194 and Val261 residues (Fig. 7C), with a docking score of −7.46 Kcal mol^{-1} and ligand efficiency of 0.48 Kcal mol^{-1}·non-hydrogen $atom^{-1}$. The selective agonist of CB2 AM12033 (Ki = 0.37 nM for CB2) which is the co-crystalized ligand of CB2 receptor and interacts through H-bond with Ser285 and hydrophobic interactions with Phe91, Phe94, Val113, Thr114, Phe117, Phe183, Pro184, Trp194, Trp258 and Val261 residues, resulting in a docking score of −10.55 Kcal mol^{-1}, RMSD of 0.80 Å and ligand efficiency of 0.36 Kcal mol^{-1}·non-hydrogen $atom^{-1}$.

The docking calculations for GPR55 suggested that S-KET binds through π-cation interaction with Phe12 and hydrophobic interactions with Ile257, Phe268, Phe269 and Leu270 (Fig. 7D), with a docking score and ligand efficiency results of −7.41 Kcal mol^{-1} and 0.46 Kcal mol^{-1}·non-hydrogen $atom^{-1}$, respectively (Table 1). Also, we performed docking calculations for a selective GPR55 agonist ML184 (EC_{50} = 250 nM) to allow a comparison standard with S-KET and it leads to a docking score of −8.91 Kcal/mol and ligand efficiency of 0.27 Kcal mol^{-1}·non-hydrogen $atom^{-1}$. ML184 binds via hydrophobic interactions with Ile257, Ile266, Phe269 and Leu272. S-KET and the ML184 agonist shared similar interactions in the GPR55 binding site.

S-KET interacts with MAGL mainly through hydrophobic interactions with Met123, Leu148, Ala151, Leu205 and Ile179 residues (Fig. 7E), with a docking score and ligand efficiency values of −6.72 Kcal mol^{-1} and 0.42 Kcal mol^{-1}·non-hydrogen $atom^{-1}$, respectively (Table 1). In the crystal structure of MAGL in complex with the inhibitor 3 l, the pyrrolidinone oxygen makes hydrogen bonds with the catalytic Ser122, Ala51 and Met123 residues; the *o*-chloro substitution interacts with Ile179; the thiazolyl carbonyl makes hydrogen bond with the Arg57, Glu53 and His272 residues, sharing some similar interactions with S-KET docking pose. The redocking calculations for the inhibitor 3 l presented a docking score of −15.08 Kcal mol^{-1}, RMSD of 0.20 Å and ligand efficiency of 0.47 Kcal mol^{-1}·non-hydrogen $atom^{-1}$.

The docking with S-KET and the FABP5 binding site suggest that S-KET made π-stacking interactions with Phe19 residue; as well H-bond with Thr56 and with water molecules (Fig. 7F), resulting in a docking score of −6.60 Kcal mol^{-1} and ligand efficiency of 0.41 Kcal mol^{-1}·non-hydrogen $atom^{-1}$. In the crystal structure of FABP5 in complex with the RO6806051 inhibitor (K_i = 86 nM), the tetrazole ring interacts with Arg129, Tyr131 or through water mediated hydrogen bonds, π-stacking

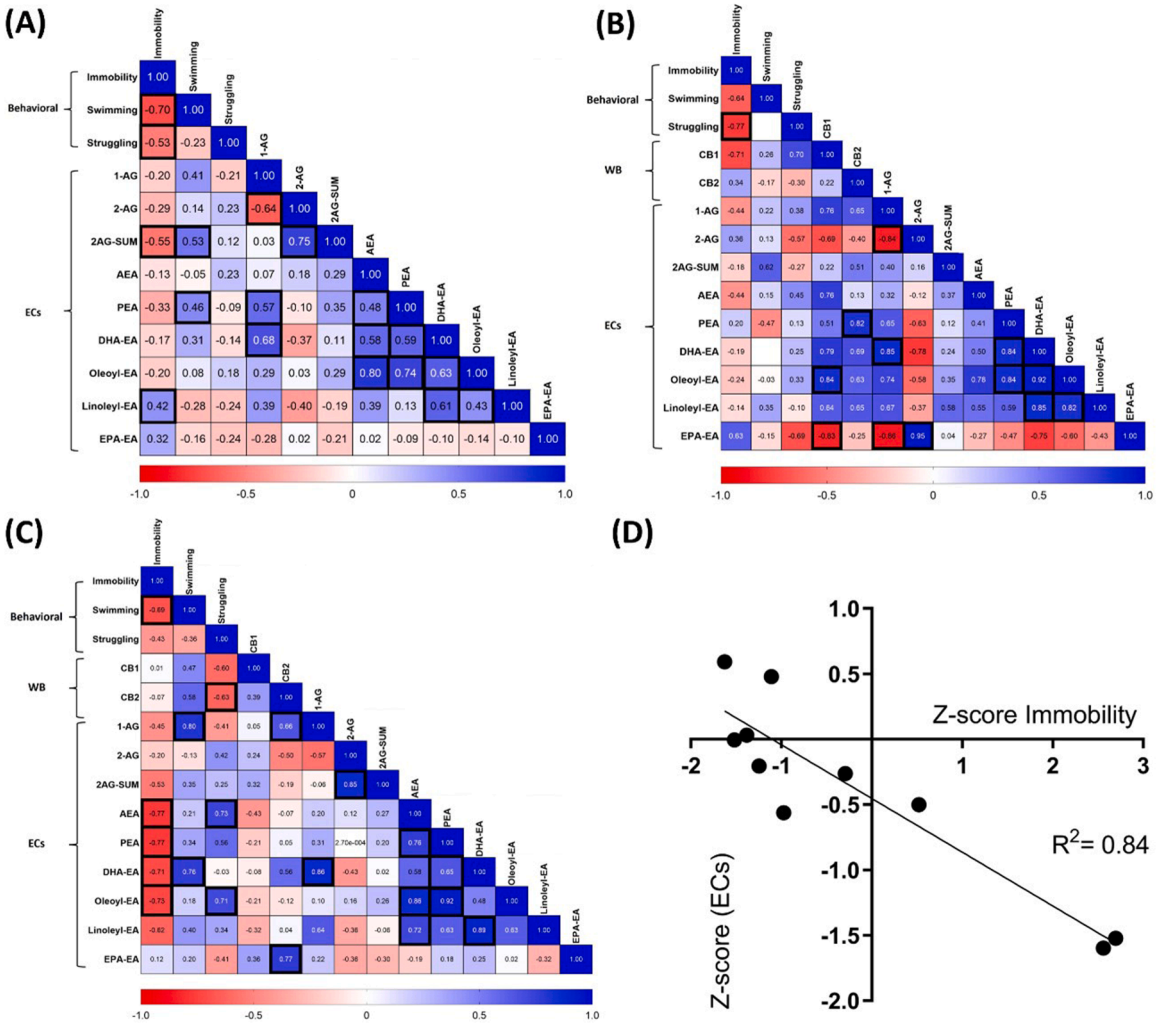

Fig. 5. Correlation of endocannabinoid levels with behavioral changes in the FST. A) Correlation of specific endocannabinoids with behavior regardless of the animals' experimental group (FRL, FSL-Sal and FSL-S-KET). (B) and (C) The behavioral data was correlated with endocannabinoids in FSL-Sal and FSL-S-KET rats, respectively, to identify possible changes associated with the drug effect. (D) Correlation of the endocannabinoid index (composite z-score of endocannabinoid changes) with the normalized immobility in FSL-S-KET reflecting significant effects of S-KET in the endocannabinoid tone. Red and blue denoted negative and positive correlation, respectively. Results of the correlation analysis expressed according to Pearson's correlation coefficient. Darker squares represent $p < 0.05$. For complete statistical analyses see Supplementary Table S2.

with Phe19 and hydrophobic interaction with Ala39, Pro41, Thr56, Ala78 and Ile107. The redocking calculations for the inhibitor RO6806051 presented a docking score of −10.72 Kcal mol^{-1} and ligand efficiency of 0.38 Kcal mol^{-1}·non-hydrogen $atom^{-1}$.

The docking score and LE results for the TRPV1 target were not satisfactory for any ligand (see Supplementary Table S3). The docking score of S-KET (-4.33 Kcal mol^{-1}) and its metabolites were higher than the docking score of TRPV1 antagonist A784168 (-4.68 Kcal mol^{-1}) and LE < 0.3 Kcal mol^{-1}·non-hydrogen $atom^{-1}$, suggesting that this is not a promising target.

4. Discussion

In the present study, we investigated the involvement of the ECS in the rapid antidepressant effect induced by S-KET in an animal model of depression based on selective breeding. Our findings revealed, for the first time, that S-KET rapidly restores the deficit in 2-AG levels in the PFC of FSL, in association with the reversal of their depression-like behavior. Although S-KET did not significantly interfere with the levels of proteins associated with the ECS, it increased the binding potential of CB1. Moreover, the antidepressant effects of S-KET in FSL were highly correlated with its ability to increase the endocannabinoid tone in their PFC, suggesting that an overall facilitation of endocannabinoid-mediated signaling may be part of its mechanism of action. However, the lack of effect of RIMO on S-KET treated groups indicates more complex interactions with the ECS, which are supported by our computational analysis showing promising binding affinity of S-KET and its metabolite (2S,6S)-HNK in several components of the ECS, notably CB1, CB2, GPR55 and FAAH.

FSL animals, known for their heightened susceptibility to stress and depressive-like behaviors, are considered valuable experimental tools for studying depression neurobiology [43]. As described by others, we observed that control FSL display increased immobility and decreased swimming in the FST when compared to their FRL counterparts, confirming their depressive-like endophenotype when exposed to an acute stressor [41]. S-KET rapidly reduced the immobility time and increased active behaviors (swimming and struggling) in the FST, corroborating previous studies showing that it induces rapid behavioral effects in FSL rats [41,88]. Importantly, S-KET effects in the FST were not due to changes in locomotor activity, as no differences between groups were observed in the OFT.

A previous study from our group detected reduced 2-AG levels in the

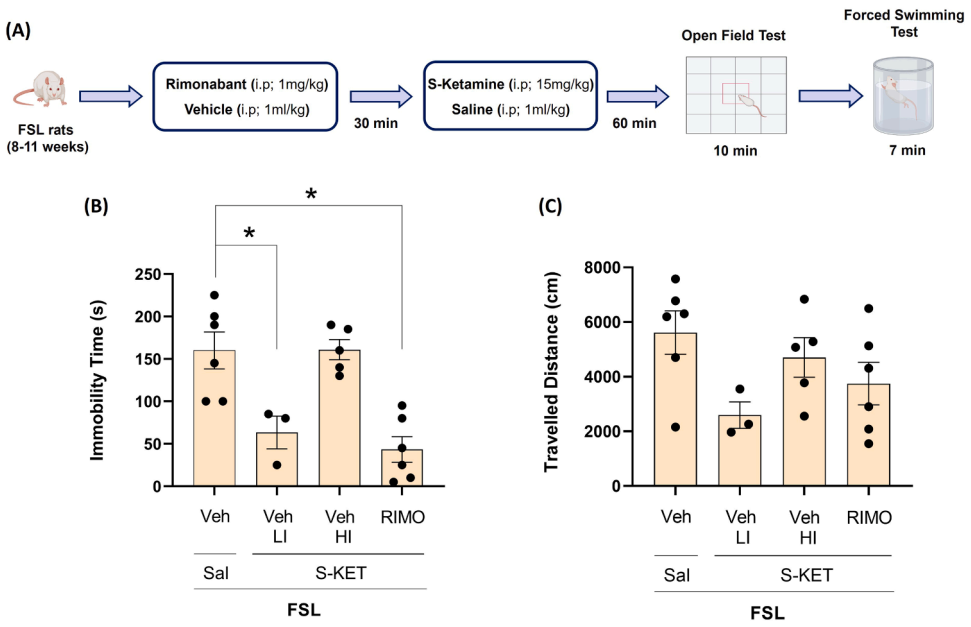

Fig. 6. Impact of the CB1 antagonist on acute treatment with S-KET in FSL rats submitted to FST and OFT. (A) Schematic diagram of the experimental design. (B) Immobility time in the FST; and (C) travelled distance in the OFT. The animals treated with Vehicle followed by S-KET were divided into two groups according to the immobility time: low immobility (LI; responder) and high immobility (HI; non-responder). Data represent the mean ± SEM. *$p < 0.05$ from FSL Veh+Sal group (One-way ANOVA followed by Tukey's post hoc); n = 3–6/group.

Table 1
Computational binding affinity prediction of S-KET in endocannabinoid system protein targets.

Target	Ligand	Docking score (Kcal mol^{-1})	Ligand efficiency (Kcal mol^{-1}·non-hydrogen $atom^{-1}$)
FAAH	**S-KET**	**−8.17**	**0.51**
FAAH	FAAH antagonist (JNJ1661010)	−9.75	0.37
CB1	**S-KET**	**−7.62**	**0.47**
CB1	CB1 agonist (AM11542)	−11.84	0.42
CB2	**S-KET**	**−7.46**	**0.46**
CB2	CB2 agonist (AM12033)	−10.54	0.36
MAGL	**S-KET**	**−6.72**	**0.42**
MAGL	MAGL inhibitor (3 l)	−15.08	0.47
GPR55	**S-KET**	**−7.41**	**0.46**
GPR55	GPR55 agonist (ML184)	−8.91	0.27
FABP5	**S-KET**	**−6.60**	**0.41**
FABP5	FAPB5 antagonist (RO6806051)	−10.72	0.38

Abbreviations: CB1: cannabinoid receptor 1; CB2: cannabinoid receptor 2; MAGL: monoacylglycerol lipase; FAAH: fatty acid amide hydrolase; GPR55: G protein-coupled receptor 55; FABP5: fatty acid binding protein 5.

PFC of naïve FSL, suggesting that impaired endocannabinoid signaling in the PFC could be an intermediate molecular endophenotype linking the increased vulnerability of FSL to stress [28]. The result of the present study adds to our previous findings by demonstrating that 2-AG levels in the PFC of FSL were negatively correlated with the depressive behavior in the FST (correlation matrix, Fig. 5A).

Under uncontrollable stress, the PFC typically exerts a top-down control over other limbic brain regions involved with the negative emotional consequences of stress, such as the basolateral amygdala (BLA) [89]. Cortical 2-AG plays a central role in this regulation by inhibiting the release of excitatory neurotransmitters in the PFC-BLA pathway, thereby dampening the negative emotional consequences induced by stress [89]. Therefore, compromised 2-AG signaling in the PFC would allow the disinhibition of this pathway and the translation of exaggerated stress responses into affective consequences, such as anxiety and depression [89]. In this scenario, the reduced levels of 2-AG in FSL could be part of a molecular endophenotype linking a previously described PFC dysregulation in FSL with their increased vulnerability to acute stress [90–93], which were reversed by S-KET. Noteworthy, other studies using different rodent models have reported contrary findings, which could reflect particularities of the species and strains used, as well as aspects of controllability and duration of the stress protocol used [94,95].

AEA levels were unaltered in the PFC of FSL and FRL rats in our study, as described in naïve FSL/FRL [28]. Since reduced levels of AEA were observed in the hippocampus of naïve FSL rats [28], it is possible that the regulation of this endocannabinoid in other brain regions could contribute to their increased vulnerability to stress and the antidepressant effect of S-KET. Curiously, even though we did not observe significant differences between groups when comparing the average of AEA in treated and untreated groups, we did find a significant correlation of the antidepressant effect of S-KET with the levels of AEA in the PFC of FSL rats. Noteworthy, in other rodent models, stress decreased cortical AEA levels in the PFC and AEA direct administration into the PFC triggered antidepressant-like effects in the FST via local CB1 receptors [96,97]. Altogether, this may reflect the a selective regulation of main endocannabinoids in the brain, depending on the stress (nature, duration) and the neurobiological differences between species/strains that account for their specific emotional responses to stress and treatment [98,99].

In addition to the classical ECS, our study screened, for the first time, changes in the levels of several other ECS in FRL and FSL, such as: 1-AG, PEA, Linoleyl-EA, DHA-EA, Oleoyl-EA, and EPA-EA. We observed a reduction in PEA levels in FSL-Sal, and a trend towards an increase in Linoleyl-EA when compared to FRL-Sal. A previous study demonstrated that there is a correlation between PEA and Linoleyl-EA blood plasma levels and the emotional response of healthy individuals [100]. In preclinical studies, treatment with PEA attenuated the depressive and cognitive deficits observed in different animal models of depression [101,102]. Accordingly, our analysis detected a correlation between PEA and swimming in FST. Altogether these results suggest a possible

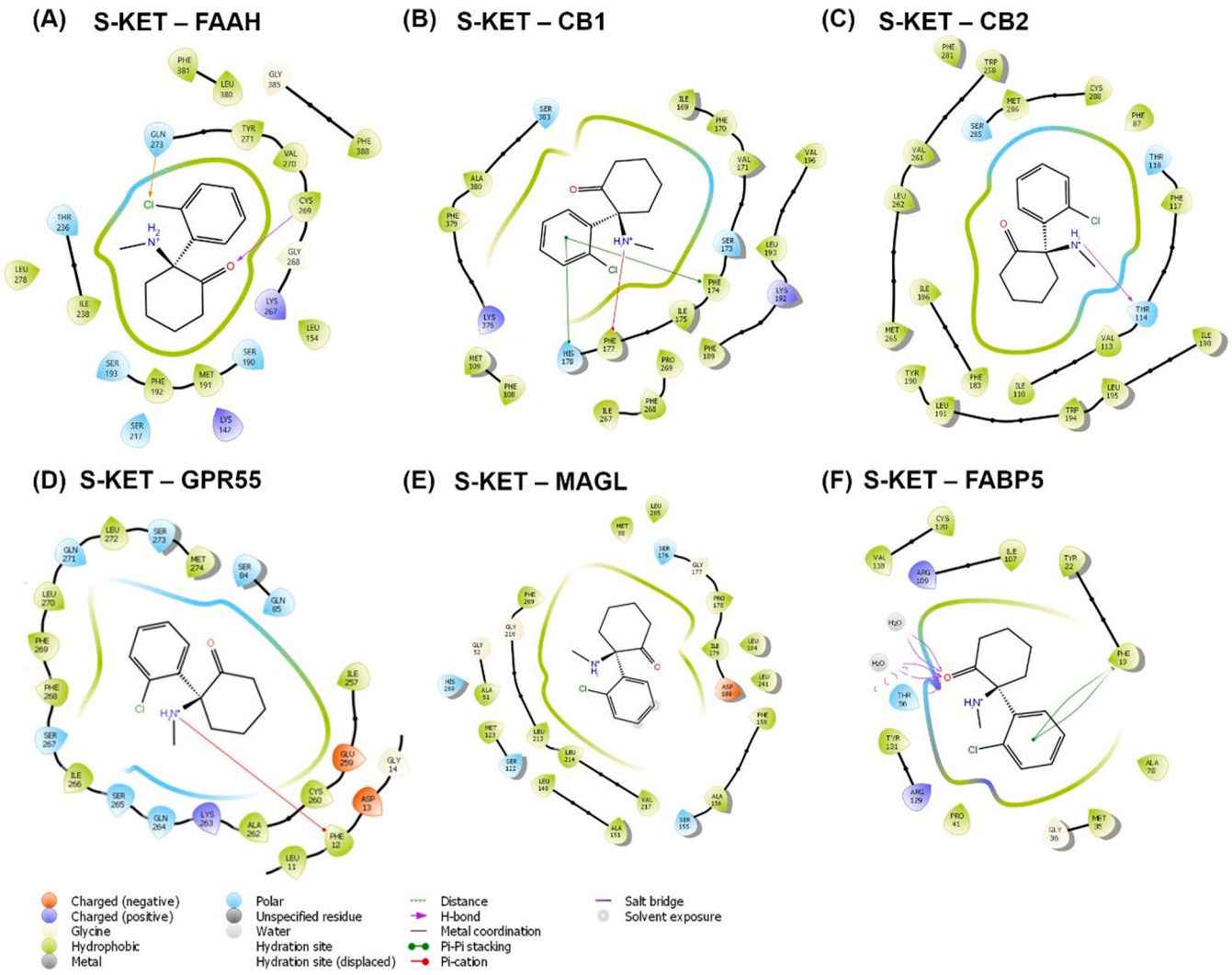

Fig. 7. Intermolecular interaction of S-KET with ECS targets. 2D interactions of S-KET with the FAAH (A) CB1 (B), CB2 (C), GPR55 (D), MAGL and FABP5 (F). H-bonds are presented as violet arrows; π-stacking interaction are presented as green lines; π-cation interactions are presented as red lines.

involvement of PEA and Linoleyl-EA in the manifestation of depressive-like behavior in this animal model of depression, which merits further investigation.

Chronic treatment with monoaminergic antidepressants, as well as non-pharmacological interventions targeting depressed mood can increase 2-AG and/or AEA levels in the PFC [103–106]. This is consistent with the proposed involvement of brain endocannabinoids in the mechanism of action of antidepressants, further supported by several studies demonstrating that the pharmacological inhibition of their enzymatic degradation (with FAAH and/or MAGL inhibitors) induces antidepressant-like effects in animal models [106,107].

Surprisingly, when evaluating S-KET effects on endocannabinoids levels in the PFC, we observed that it only slightly reversed the reduction in cortical 2-AG levels in FSL rats, without affecting other endocannabinoids. However, the magnitude of S-KET effect in the FST was strongly correlated with an increase in AEA levels and in the overall endocannabinoid signaling in the PFC. This suggests that the behavioral effects of S-KET in FSL may arise from an additive mechanism that results from a concomitant modulation of multiple endocannabinoids in the PFC, thereby producing an increased local endocannabinoid tone. Previous research has shown that decreased endocannabinoid levels in the PFC is associated with depressive-like behavior in different stress models [108–110]. Activation of CB1 receptors in the PFC leads to disinhibition of the dorsal raphe nucleus (DRN) through a polysynaptic circuit, resulting in increased serotonin release in the PFC [111–113], which is required for ketamine effects [114]. Therefore, S-KET antidepressant effect could result from an endocannabinoid-dependent regulation of serotonin signaling in the PFC.

To further clarify S-KET effects in the cortical ECS, we assessed the transcript and protein levels of main receptors and of the enzymes responsible for the degradation of 2-AG and AEA, which can directly affect their bioavailability at the synapses [115]. We observed a significant increase in FAAH and CB1 gene expression in the FSL-Sal compared to FRL-Sal, which were attenuated by S-KET, but without corresponding changes at the protein levels in the western blot. Since this technique does not differentiate between receptors available for binding (at the membrane) or internalized (in the cytosol), we evaluated S-KET effect on CB1 binding using a radiolabeled CB1-binding drug. Our results suggest that S-KET slightly increases CB1 binding to the radiolabeled drug in the PFC of FSL, which could reflect changes in the receptor number and/or its affinity states [116]. Chronic, but not acute, treatment with monoaminergic antidepressants also increase drug binding to CB1 receptors, particularly in the rodent PFC [117], although contradictory results are reported depending on the drug type and the model used [118–120]. Therefore, it is likely that S-KET rapidly regulates CB1 signaling in the PFC, but our small sample size and the lack of evaluation of CB1 levels in different cell types may have hindered more robust differences in our results [121,122].

We then considered whether blocking CB1 receptors with RIMO could inhibit the antidepressant-like effects of S-KET. For the vehicle-treated animals, we noticed a higher variability in our data, with two clusters with distinct behavioral responses to S-KET. We divided these animals into responders to S-KET treatment (Veh-LI-KET) and non-responders (Veh-HI-KET) instead of repeating the experiment to avoid the unnecessary use of additional animals. In the animals treated with RIMO and S-KET, we did not observe a similar cluster separation, with animals in this group presenting LI. This indicates that, rather than blocking S-KET effects in the FST, RIMO seemed to facilitate its antidepressant properties. Although surprising, previous studies from our laboratory have shown that the psychostimulant effects induced by S-KET were absent in mice with pharmacological or genetic inhibition of CB1- signaling, but not its antidepressant properties in unstressed mice exposed to the FST [39]. Furthermore, other studies suggest that systemic administration of RIMO has no effect or decrease immobility time in the FST [123–125].

Since RIMO was systemically administered, its lack of effect could result from compensatory mechanisms arising from contrasting modulatory actions of CB1 receptors located in different brain regions. For example, while CB1 activation in the PFC disinhibits the firing of serotonergic neurons in the DRN and triggers a serotonin-dependent antidepressant effect [112,126,127], CB1 activation in the DRN inhibits serotonergic neurons and serotonin release in the PFC [128], which is essential for stress adaptation and mood regulation [112,127]. Based on that, we could speculate that the blockage of CB1 in the DRN by RIMO would increase serotonergic firing and serotonin release in the forebrain, including the PFC, leaving S-KET effects unaltered despite the blockade of CB1 in the PFC. Supporting this perspective, there is evidence that the antidepressant effect of KET is dependent on serotonin availability [129] and 5-HT1A receptor activation in the PFC [130]; while RIMO facilitates the antidepressant effect of SSRIs [131]. Nevertheless, this hypothesis warrants further investigation.

To inquire if S-KET effects could involve the modulation of other targets of the ECS, we performed computational predictions to estimate the binding affinity of S-KET and its metabolites for the different components of the ECS. Our data suggested that both S-KET and its derived metabolites, 2S,6S-HNK and S-NORK, showed promising affinity and binding profiles to several targets of this system, such as FAAH, CB2 and GPR55, and for the enzyme MAGL in the case of the 2S,6S-HNK metabolite. Although these results were not directly confirmed in vitro (except the CB1 binding), our data indicates that the effects of KET may arise from its combined action on multiple components of the ECS.

Our study presents important limitations. The predicted affinity of S-KET for the receptors does not allow us to determine about the underlining mechanisms (blockade or activation), which requires further investigation with multiple binding assays and evaluation of enzymatic activity. On the note, we assessed S-KET effects at only one time-point (1 h, acute), and it is possible that more robust changes in the ECS would be observed in association with its sustained or prolonged effects. Moreover, additional animal models based on chronic exposure to stress could provide valuable information about the involvement of the ECS in S-KET antidepressant effects. Another imitation is the lack of analyses of enzyme activity, which could help us understand if S-KET regulates eCB levels by regulating their degradation. Finally, we did not evaluate S-KET effects in female rats, which could be a source of important information, despite evidence of no differences in responding to S-KET between female and male FSL [55]. Nevertheless, our findings are innovative by demonstrating that the rapid antidepressant effect of S-KET involves the ECS regulation in the PFC, raising the possibility to explore if augmenting ECS in this brain region could rapidly alleviate depressive-like behaviors.

5. Conclusions

Our study showed that the antidepressant effect of S-KET in FSL rats, a well-validated animal model of depression, is potentially associated with the regulation of the endocannabinoid tone in the PFC. It is also possible that S-KET (and its metabolites) directly regulate other targets of the ECS, such as FABP5, FAAH and MAGL. Further research is necessary to clarify the relevance of each of these targets in mediating S-KET's effects and how they can collectively contribute to triggering rapid antidepressant effects. Studies with local inhibition of eCB signaling in the PFC can help understanding the biological significance of our findings for S-KET actions.

CRediT authorship contribution statement

Anne M. Landau: Writing – review & editing, Resources. **Carolina H. Andrade:** Writing – review & editing. **Pedro H. Gobira:** Writing – review & editing, Investigation. **Alessio Nicola Ferraro:** Writing – review & editing, Investigation. **Caroline C. Real:** Writing – review & editing, Investigation. **Anna L. Waszkiewicz:** Writing – review & editing, Investigation. **Melina Mottin:** Writing – review & editing, Investigation, Formal analysis. **Sâmia R.L. Joca:** Writing – review & editing, Supervision, Project administration, Funding acquisition, Data curation, Conceptualization. **Luana B. Domingos:** Writing – review & editing, Investigation. **Adriano M. Chaves-Filho:** Writing – review & editing, Investigation, Formal analysis. **Heidi K. Muller:** Writing – review & editing, Resources, Investigation. **Nicole R. Silva:** Writing – review & editing, Writing – original draft, Methodology, Investigation, Formal analysis, Data curation, Conceptualization. **Gregers Wegener:** Writing – review & editing, Resources. **Shokouh Arjmand:** Writing – review & editing, Investigation, Formal analysis.

Funding

This study was supported by Aarhus University Research Foundation, Denmark (grant number: AUFF-E 2020-7-1 9), Jascha Foundation, Denmark (grant number: 2023-0381) and FAPESP, Brazil (2017/24304-0). SJ is currently supported by Lundbeck Foundation, Denmark (grant number: R366-2021-255). SJ received an AIAS-Cofund fellowship (Marie Curie Fellowship), sponsored by The European Union Horizon 2020 (grant agreement 754513), during the conceptualization phase of the study (2019-2020).

Declaration of Competing Interest

The manuscript has been read and approved by all authors and there are no other persons who satisfied the criteria for authorship but are not listed. We further confirm that the order of authors listed in the manuscript has been approved by all of us. The authors declare that they have no known competing financial interests or personal relationships that could have appeared to influence the work reported in this paper.

Acknowledgment

The authors express their gratitude to Tania Aaquist Ammitzbøll, Per Fuglsang Mikkelsen and Jayashree Sahana for their technical support.

Appendix A. Supporting information

Supplementary data associated with this article can be found in the online version at doi:10.1016/j.phrs.2024.107545.

Data availability

All data is available through an DOI mentioned in the manuscript

References

[1] C. Otte, S.M. Gold, B.W. Penninx, C.M. Pariante, A. Etkin, M. Fava, D.C. Mohr, A. F. Schatzberg, Major depressive disorder, Nat. Rev. Dis. Prim. 2 (2016) 16065, https://doi.org/10.1038/nrdp.2016.65.

[2] A. DiBernardo, X. Lin, Q. Zhang, J. Xiang, L. Lu, C. Jamieson, C. Benson, K. Lee, R. Bodén, L. Brandt, P. Brenner, J. Reutfors, G. Li, Humanistic outcomes in treatment resistant depression: a secondary analysis of the STAR*D study, BMC Psychiatry 18 (2018) 352, https://doi.org/10.1186/s12888-018-1920-7.

[3] K.S. Kendler, C.O. Gardner, C.A. Prescott, Toward a comprehensive developmental model for major depression in men, Am. J. Psychiatry 163 (2006) 115–124, https://doi.org/10.1176/appi.ajp.163.1.115.

[4] M.F. Juruena, R. Gadelrab, A.J. Cleare, A.H. Young, Epigenetics: a missing link between early life stress and depression, Prog. Neuropsychopharmacol. Biol. Psychiatry 109 (2021) 110231, https://doi.org/10.1016/j.pnpbp.2020.110231.

[5] A. Du Preez, J. Eum, I. Eiben, P. Eiben, P.A. Zunszain, C.M. Pariante, S. Thuret, C. Fernandes, Do different types of stress differentially alter behavioural and neurobiological outcomes associated with depression in rodent models? A systematic review, Front. Neuroendocr. 61 (2021) 100896, https://doi.org/10.1016/j.yfrne.2020.100896.

[6] D.A. Morilak, A. Frazer, Antidepressants and brain monoaminergic systems: a dimensional approach to understanding their behavioural effects in depression and anxiety disorders, Int. J. Neuropsychopharmacol. 7 (2004) 193–218, https://doi.org/10.1017/S1461145704004080.

[7] A.J. Rush, M. Fava, S.R. Wisniewski, P.W. Lavori, M.H. Trivedi, H.A. Sackeim, M. E. Thase, A.A. Nierenberg, F.M. Quitkin, T.M. Kashner, D.J. Kupfer, J. F. Rosenbaum, J. Alpert, J.W. Stewart, P.J. McGrath, M.M. Biggs, K. Shores-Wilson, B.D. Lebowitz, L. Ritz, G. Niederehe, for the STAR*D Investigators Group, Sequenced treatment alternatives to relieve depression (STAR*D): rationale and design, Control Clin. Trials 25 (2004) 119–142, https://doi.org/10.1016/S0197-2456(03)00112-0.

[8] D.J. Kupfer, E. Frank, M.L. Phillips, Major depressive disorder: new clinical, neurobiological, and treatment perspectives, Focus (Madison) 14 (2016) 266–276, https://doi.org/10.1176/appi.focus.140208.

[9] D. Richards, Prevalence and clinical course of depression: a review, Clin. Psychol. Rev. 31 (2011) 1117–1125, https://doi.org/10.1016/j.cpr.2011.07.004.

[10] D.L. Dunner, A.J. Rush, J.M. Russell, M. Burke, S. Woodard, P. Wingard, J. Allen, Prospective, long-term, multicenter study of the naturalistic outcomes of patients with treatment-resistant depression, J. Clin. Psychiatry 67 (2006) 688–695, https://doi.org/10.4088/JCP.v67n0501.

[11] X. Gonda, P. Dome, J.C. Neill, F.I. Tarazi, Novel antidepressant drugs: beyond monoamine targets, CNS Spectr. 28 (2023) 6–15, https://doi.org/10.1017/S1092852921000791.

[12] S. Kohtala, Ketamine—50 years in use: from anesthesia to rapid antidepressant effects and neurobiological mechanisms, Pharmacol. Rep. 73 (2021) 323–345, https://doi.org/10.1007/s43440-021-00232-4.

[13] J.H. Krystal, E.T. Kavalali, L.M. Monteggia, Ketamine and rapid antidepressant action: new treatments and novel synaptic signaling mechanisms, Neuropsychopharmacol 49 (2024) 41–50, https://doi.org/10.1038/s41386-023-01629-w.

[14] B. Sanders, A.Q. Brula, Intranasal esketamine: from origins to future implications in treatment-resistant depression, J. Psychiatr. Res. 137 (2021) 29–35, https://doi.org/10.1016/j.jpsychires.2021.02.020.

[15] S. Chaki, M. Watanabe, Antidepressants in the post-ketamine Era: pharmacological approaches targeting the glutamatergic system, Neuropharmacology 223 (2023) 109348, https://doi.org/10.1016/j.neuropharm.2022.109348.

[16] G. Sanacora, Z. Yan, M. Popoli, The stressed synapse 2.0: pathophysiological mechanisms in stress-related neuropsychiatric disorders, Nat. Rev. Neurosci. 23 (2022) 86–103, https://doi.org/10.1038/s41583-021-00540-x.

[17] P. Zanos, T.D. Gould, Mechanisms of ketamine action as an antidepressant, Mol. Psychiatry 23 (2018) 801–811, https://doi.org/10.1038/mp.2017.255.

[18] T.H. Pham, A.M. Gardier, Fast-acting antidepressant activity of ketamine: highlights on brain serotonin, glutamate, and GABA neurotransmission in preclinical studies, Pharmacol. Ther. 199 (2019) 58–90, https://doi.org/10.1016/j.pharmthera.2019.02.017.

[19] S. Deyama, R.S. Duman, Neurotrophic mechanisms underlying the rapid and sustained antidepressant actions of ketamine, Pharmacol. Biochem. Behav. 188 (2020) 172837, https://doi.org/10.1016/j.pbb.2019.172837.

[20] P. Kowiański, G. Lietzau, E. Czuba, M. Waśkow, A. Steliga, J. Moryś, BDNF: a key factor with multipotent impact on brain signaling and synaptic plasticity, Cell. Mol. Neurobiol. 38 (2018) 579–593, https://doi.org/10.1007/s10571-017-0510-4.

[21] K. Fukumoto, M. Iijima, T. Funakoshi, S. Chaki, Role of 5-HT1A receptor stimulation in the medial prefrontal cortex in the sustained antidepressant effects of ketamine, Int. J. Neuropsychopharmacol. 21 (2018) 371–381, https://doi.org/10.1093/ijnp/pyx116.

[22] K.G. du Jardin, N. Liebenberg, M. Cajina, H.K. Müller, B. Elfving, C. Sanchez, G. Wegener, S-ketamine mediates its acute and sustained antidepressant-like activity through a 5-HT1B receptor dependent mechanism in a genetic rat model of depression, Front. Pharmacol. 8 (2018), https://doi.org/10.3389/fphar.2017.00978.

[23] P.C. Casarotto, M. Girych, S.M. Fred, V. Kovaleva, R. Moliner, G. Enkavi, C. Biojone, C. Cannarozzo, M.P. Sahu, K. Kaurinkoski, C.A. Brunello, A. Steinzeig, F. Winkel, S. Patil, S. Vestring, T. Serchov, C.R.A.F. Diniz, L. Laukkanen, I. Cardon, H. Antila, T. Rog, T.P. Piepponen, C.R. Bramham, C. Normann, S. E. Lauri, M. Saarma, I. Vattulainen, E. Castrén, Antidepressant drugs act by directly binding to TRKB neurotrophin receptors, Cell 184 (2021) 1299–1313. e19, https://doi.org/10.1016/j.cell.2021.01.034.

[24] R.C.M. Ferreira, M.G.M. Castor, F. Piscitelli, V. Di Marzo, I.D.G. Duarte, T.R. L. Romero, The involvement of the endocannabinoid system in the peripheral antinociceptive action of ketamine, J. Pain. 19 (2018) 487–495, https://doi.org/10.1016/j.jpain.2017.12.002.

[25] W. Xu, H. Li, L. Wang, J. Zhang, C. Liu, X. Wan, X. Liu, Y. Hu, Q. Fang, Y. Xiao, Q. Bu, H. Wang, J. Tian, Y. Zhao, X. Cen, Endocannabinoid signaling regulates the reinforcing and psychostimulant effects of ketamine in mice, Nat. Commun. 11 (2020) 5962, https://doi.org/10.1038/s41467-020-19780-z.

[26] H.-C. Lu, K. Mackie, Review of the endocannabinoid system, Biol. Psychiatry Cogn. Neurosci. Neuroimaging 6 (2021) 607–615, https://doi.org/10.1016/j.bpsc.2020.07.016.

[27] B. Dong, B.M. Shilpa, R. Shah, A. Goyal, S. Xie, M.J. Bakalian, R.F. Suckow, T. B. Cooper, J.J. Mann, V. Arango, K.Y. Vinod, Dual pharmacological inhibitor of endocannabinoid degrading enzymes reduces depressive-like behavior in female rats, J. Psychiatr. Res. 120 (2020) 103–112, https://doi.org/10.1016/j.jpsychires.2019.10.010.

[28] C. Kirkedal, B. Elfving, H.K. Müller, F.A. Moreira, L. Bindila, B. Lutz, G. Wegener, N. Liebenberg, Hemisphere-dependent endocannabinoid system activity in prefrontal cortex and hippocampus of the Flinders Sensitive Line rodent model of depression, Neurochem. Int. 125 (2019) 7–15, https://doi.org/10.1016/j.neuint.2019.01.023.

[29] M.N. Hill, G.E. Miller, E.J. Carrier, B.B. Gorzalka, C.J. Hillard, Circulating endocannabinoids and N-acyl ethanolamines are differentially regulated in major depression and following exposure to social stress, Psychoneuroendocrinology 34 (2009) 1257–1262, https://doi.org/10.1016/j.psyneuen.2009.03.013.

[30] I. Gallego-Landin, A. García-Baos, A. Castro-Zavala, O. Valverde, Reviewing the role of the endocannabinoid system in the pathophysiology of depression, Front. Pharmacol. 12 (2021), https://doi.org/10.3389/fphar.2021.762738.

[31] D. Zhou, Y. Li, T. Tian, W. Quan, L. Wang, Q. Shao, L.Q. Fu, X.H. Zhang, X. Y. Wang, H. Zhang, Y.M. Ma, Role of the endocannabinoid system in the formation and development of depression, Pharmazie 72 (2017) 435–439, https://doi.org/10.1691/ph.2017.7474.

[32] A. King, Neuropsychiatric adverse effects signal the end of the line for rimonabant, Nat. Rev. Cardiol. 7 (2010), https://doi.org/10.1038/nrcardio.2010.148, 602–602.

[33] P. Paudel, S. Ross, X.-C. Li, Molecular targets of cannabinoids associated with depression, Curr. Med. Chem. 29 (2022) 1827–1850, https://doi.org/10.2174/0929867328666210623144658.

[34] U. Bright, I. Akirav, Modulation of endocannabinoid system components in depression: pre-clinical and clinical evidence, Int. J. Mol. Sci. 23 (2022) 5526, https://doi.org/10.3390/ijms23105526.

[35] V. Micale, K. Tabiova, J. Kucerova, F. Drago, Role of the endocannabinoid system in depression: from preclinical to clinical evidence, in: Cannabinoid Modulation of Emotion, Memory, and Motivation, Springer New York, New York, NY, 2015, pp. 97–129, 10.1007/978-1-4939-2294-9_5.

[36] L.J.A. Durieux, S.R.J. Gilissen, L. Arckens, Endocannabinoids and cortical plasticity: CB1R as a possible regulator of the excitation/inhibition balance in health and disease, Eur. J. Neurosci. 55 (2022) 971–988, https://doi.org/10.1111/ejn.15110.

[37] K.M. Silveira, G. Wegener, S.R.L. Joca, Targeting 2-arachidonoylglycerol signalling in the neurobiology and treatment of depression, Basic Clin. Pharmacol. Toxicol. 129 (2021) 3–14, https://doi.org/10.1111/bcpt.13595.

[38] W. Xu, H. Li, L. Wang, J. Zhang, C. Liu, X. Wan, X. Liu, Y. Hu, Q. Fang, Y. Xiao, Q. Bu, H. Wang, J. Tian, Y. Zhao, X. Cen, Endocannabinoid signaling regulates the reinforcing and psychostimulant effects of ketamine in mice, Nat. Commun. 11 (2020) 5962, https://doi.org/10.1038/s41467-020-19780-z.

[39] P.H. Gobira, J. LaMar, J. Marques, A. Sartim, K. Silveira, L. Santos, G. Wegener, F. S. Guimaraes, K. Mackie, H.-C. Lu, S. Joca, CB1 receptor silencing attenuates ketamine-induced hyperlocomotion without compromising its antidepressant-like effects, Cannabis Cannabinoid Res. 8 (2023) 768–778, https://doi.org/10.1089/can.2022.0072.

[40] A.P.M. Lullau, E.M.W. Haga, E.H. Ronold, G.E. Dwyer, Antidepressant mechanisms of ketamine: a review of actions with relevance to treatment-resistance and neuroprogression, Front. Neurosci. 17 (2023), https://doi.org/10.3389/fnins.2023.1223145.

[41] K.G. du Jardin, N. Liebenberg, M. Cajina, H.K. Müller, B. Elfving, C. Sanchez, G. Wegener, S-Ketamine mediates its acute and sustained antidepressant-like activity through a 5-HT1B receptor dependent mechanism in a genetic rat model of depression, Front. Pharmacol. 8 (2018), https://doi.org/10.3389/fphar.2017.00978.

[42] D.H. Overstreet, E. Friedman, A.A. Mathé, G. Yadid, The Flinders Sensitive Line rat: a selectively bred putative animal model of depression, Neurosci. Biobehav. Rev. 29 (2005) 739–759, https://doi.org/10.1016/j.neubiorev.2005.03.015.

[43] D.H. Overstreet, G. Wegener, The flinders sensitive line rat model of depression-25 years and still producing, Pharmacol. Rev. 65 (2013) 143–155, https://doi.org/10.1124/pr.111.005397.

[44] L.M. Riggs, T.D. Gould, Ketamine and the future of rapid-acting antidepressants, Annu. Rev. Clin. Psychol. 17 (2021) 207–231, https://doi.org/10.1146/annurev-clinpsy-072120-014126.

[45] Y. Fang, P. Guo, L. Lv, M. Feng, H. Wang, G. Sun, S. Wang, M. Qian, H. Chen, Scopolamine augmentation for depressive symptoms and cognitive functions in treatment-resistant depression: a case series, Asian J. Psychiatr. 82 (2023) 103484, https://doi.org/10.1016/j.ajp.2023.103484.

[46] S. Liu, D. Shi, Z. Sun, Y. He, J. Yang, G. Wang, M2-AChR Mediates rapid antidepressant effects of scopolamine through activating the mTORC1-BDNF signaling pathway in the medial prefrontal cortex, Front. Psychiatry 12 (2021), https://doi.org/10.3389/fpsyt.2021.601985.
[47] Y. Wei, L. Chang, K. Hashimoto, A historical review of antidepressant effects of ketamine and its enantiomers, Pharmacol. Biochem. Behav. 190 (2020) 172870, https://doi.org/10.1016/j.pbb.2020.172870.
[48] L.A. Jelen, A.H. Young, J.M. Stone, Ketamine: a tale of two enantiomers, J. Psychopharmacol. 35 (2021) 109–123, https://doi.org/10.1177/0269881120959644.
[49] Y. Alnefeesi, D. Chen-Li, E. Krane, M.Y. Jawad, N.B. Rodrigues, F. Ceban, J.D. Di Vincenzo, S. Meshkat, R.C.M. Ho, H. Gill, K.M. Teopiz, B. Cao, Y. Lee, R. S. McIntyre, J.D. Rosenblat, Real-world effectiveness of ketamine in treatment-resistant depression: a systematic review & meta-analysis, J. Psychiatr. Res. 151 (2022) 693–709, https://doi.org/10.1016/j.jpsychires.2022.04.037.
[50] W.S. Marcantoni, B.S. Akoumba, M. Wassef, J. Mayrand, H. Lai, S. Richard-Devantoy, S. Beauchamp, A systematic review and meta-analysis of the efficacy of intravenous ketamine infusion for treatment resistant depression: January 2009 – January 2019, J. Affect. Disord. 277 (2020) 831–841, https://doi.org/10.1016/j.jad.2020.09.007.
[51] G.P. Silote, M.C. Gatto, A. Eskelund, F.S. Guimarães, G. Wegener, S.R.L. Joca, Strain-, sex-, and time-dependent antidepressant-like effects of cannabidiol, Pharmaceuticals 14 (2021), https://doi.org/10.3390/ph14121269.
[52] K.G. du Jardin, N. Liebenberg, H.K. Müller, B. Elfving, C. Sanchez, G. Wegener, Differential interaction with the serotonin system by S-ketamine, vortioxetine, and fluoxetine in a genetic rat model of depression, Psychopharmacology 233 (2016) 2813–2825, https://doi.org/10.1007/s00213-016-4327-5.
[53] M. Ardalan, A.H. Rafati, J.R. Nyengaard, G. Wegener, Rapid antidepressant effect of ketamine correlates with astroglial plasticity in the hippocampus, Br. J. Pharmacol. 174 (2017) 483–492, https://doi.org/10.1111/bph.13714.
[54] A.J. Sales, M.V. Fogaça, A.G. Sartim, V.S. Pereira, G. Wegener, F.S. Guimarães, S. R.L. Joca, Cannabidiol induces rapid and sustained antidepressant-like effects through increased BDNF signaling and synaptogenesis in the prefrontal cortex, Mol. Neurobiol. 56 (2019) 1070–1081, https://doi.org/10.1007/s12035-018-1143-4.
[55] S. Arjmand, M.V. Pedersen, N.R. Silva, A.M. Landau, S. Joca, G. Wegener, Sex and estrous cycle are not mediators of S-ketamine's rapid-antidepressant behavioral effects in a genetic rat model of depression, Int. J. Neuropsychopharmacol. 26 (2023) 350–358, https://doi.org/10.1093/ijnp/pyad016.
[56] G. Treccani, M. Ardalan, F. Chen, L. Musazzi, M. Popoli, G. Wegener, J. R. Nyengaard, H.K. Müller, S-ketamine reverses hippocampal dendritic spine deficits in flinders sensitive line rats within 1h of administration, Mol. Neurobiol. 56 (2019) 7368–7379, https://doi.org/10.1007/s12035-019-1613-3.
[57] L.B. Domingos, H.K. Müller, N.R. da Silva, M.D. Filiou, A.L. Nielsen, F. S. Guimarães, G. Wegener, S. Joca, Repeated cannabidiol treatment affects neuroplasticity and endocannabinoid signaling in the prefrontal cortex of the Flinders Sensitive Line (FSL) rat model of depression, Neuropharmacol 248 (2024) 109870, https://doi.org/10.1016/j.neuropharm.2024.109870.
[58] K.J. Livak, T.D. Schmittgen, Analysis of relative gene expression data using real-time quantitative PCR and the 2-ΔΔCT method, Methods 25 (2001) 402–408, https://doi.org/10.1006/meth.2001.1262.
[59] H.K. Müller, A guide to analysis of relative synaptic protein abundance by quantitative fluorescent western blotting, in: Methods in Molecular Biology, Humana Press, New York, NY, 2022, pp. 89–98, https://doi.org/10.1007/978-1-0716-1916-2_7.
[60] M. Schäfer, K.R. Kakularam, F. Reisch, M. Rothe, S. Stehling, D. Heydeck, G. P. Püschel, H. Kuhn, Male knock-in mice expressing an arachidonic acid lipoxygenase 15B (Alox15B) with humanized reaction specificity are prematurely growth arrested when aging, Biomedicines 10 (2022), https://doi.org/10.3390/biomedicines10061379.
[61] K.H. Binda, A.M. Landau, M. Chacur, D.J. Brooks, C.C. Real, Treadmill exercise modulates nigral and hippocampal cannabinoid receptor type 1 in the 6-OHDA model of Parkinson's disease, Brain Res. 1814 (2023) 148436, https://doi.org/10.1016/j.brainres.2023.148436.
[62] H.M. Berman, The protein data bank, Nucleic Acids Res. 28 (2000) 235–242, https://doi.org/10.1093/nar/28.1.235.
[63] S.K. Burley, C. Bhikadiya, C. Bi, S. Bittrich, H. Chao, L. Chen, P.A. Craig, G. V. Crichlow, K. Dalenberg, J.M. Duarte, S. Dutta, M. Fayazi, Z. Feng, J.W. Flatt, S. Ganesan, S. Ghosh, D.S. Goodsell, R.K. Green, V. Guranovic, J. Henry, B. P. Hudson, I. Khokhriakov, C.L. Lawson, Y. Liang, R. Lowe, E. Peisach, I. Persikova, D.W. Piehl, Y. Rose, A. Sali, J. Segura, M. Sekharan, C. Shao, B. Vallat, M. Voigt, B. Webb, J.D. Westbrook, S. Whetstone, J.Y. Young, A. Zalevsky, C. Zardecki, RCSB Protein Data Bank (RCSB.org): delivery of experimentally-determined PDB structures alongside one million computed structure models of proteins from artificial intelligence/machine learning, Nucleic Acids Res. 51 (2023) D488–D508, https://doi.org/10.1093/nar/gkac1077.
[64] T. Hua, K. Vemuri, S.P. Nikas, R.B. Laprairie, Y. Wu, L. Qu, M. Pu, A. Korde, S. Jiang, J.-H. Ho, G.W. Han, K. Ding, X. Li, H. Liu, M.A. Hanson, S. Zhao, L. M. Bohn, A. Makriyannis, R.C. Stevens, Z.-J. Liu, Crystal structures of agonist-bound human cannabinoid receptor CB1, Nature 547 (2017) 468–471, https://doi.org/10.1038/nature23272.
[65] T. Hua, X. Li, L. Wu, C. Iliopoulos-Tsoutsouvas, Y. Wang, M. Wu, L. Shen, C. A. Brust, S.P. Nikas, F. Song, X. Song, S. Yuan, Q. Sun, Y. Wu, S. Jiang, T.W. Grim, O. Benchama, E.L. Stahl, N. Zvonok, S. Zhao, L.M. Bohn, A. Makriyannis, Z.-J. Liu, Activation and signaling mechanism revealed by cannabinoid receptor-Gi complex structures, Cell 180 (2020) 655–665.e18, https://doi.org/10.1016/j.cell.2020.01.008.
[66] H. Kühne, U. Obst-Sander, B. Kuhn, A. Conte, S.M. Ceccarelli, W. Neidhart, M. G. Rudolph, G. Ottaviani, R. Gasser, S.-S. So, S. Li, X. Zhang, L. Gao, M. Myers, Design and synthesis of selective, dual fatty acid binding protein 4 and 5 inhibitors, Bioorg. Med Chem. Lett. 26 (2016) 5092–5097, https://doi.org/10.1016/j.bmcl.2016.08.071.
[67] J. Aida, M. Fushimi, T. Kusumoto, H. Sugiyama, N. Arimura, S. Ikeda, M. Sasaki, S. Sogabe, K. Aoyama, T. Koike, Design, Synthesis, and evaluation of piperazinyl pyrrolidin-2-ones as a novel series of reversible monoacylglycerol lipase inhibitors, J. Med Chem. 61 (2018) 9205–9217, https://doi.org/10.1021/acs.jmedchem.8b00824.
[68] J. Jumper, R. Evans, A. Pritzel, T. Green, M. Figurnov, O. Ronneberger, K. Tunyasuvunakool, R. Bates, A. Žídek, A. Potapenko, A. Bridgland, C. Meyer, S. A.A. Kohl, A.J. Ballard, A. Cowie, B. Romera-Paredes, S. Nikolov, R. Jain, J. Adler, T. Back, S. Petersen, D. Reiman, E. Clancy, M. Zielinski, M. Steinegger, M. Pacholska, T. Berghammer, S. Bodenstein, D. Silver, O. Vinyals, A.W. Senior, K. Kavukcuoglu, P. Kohli, D. Hassabis, Highly accurate protein structure prediction with AlphaFold, Nature 596 (2021) 583–589, https://doi.org/10.1038/s41586-021-03819-2.
[69] M. Kim, N.J. Sisco, J.K. Hilton, C.M. Montano, M.A. Castro, B.R. Cherry, M. Levitus, W.D. Van Horn, Evidence that the TRPV1 S1-S4 membrane domain contributes to thermosensing, Nat. Commun. 11 (2020) 4169, https://doi.org/10.1038/s41467-020-18026-2.
[70] J. Ko, H. Park, L. Heo, C. Seok, GalaxyWEB server for protein structure prediction and refinement, Nucleic Acids Res. 40 (2012) W294–W297, https://doi.org/10.1093/nar/gks493.
[71] G. Madhavi Sastry, M. Adzhigirey, T. Day, R. Annabhimoju, W. Sherman, Protein and ligand preparation: parameters, protocols, and influence on virtual screening enrichments, J. Comput. Aided Mol. Des. 27 (2013) 221–234, https://doi.org/10.1007/s10822-013-9644-8.
[72] G.A. Kaminski, R.A. Friesner, J. Tirado-Rives, W.L. Jorgensen, Evaluation and reparametrization of the OPLS-AA force field for proteins via comparison with accurate quantum chemical calculations on peptides, J. Phys. Chem. B 105 (2001) 6474–6487, https://doi.org/10.1021/jp003919d.
[73] J.C. Shelley, A. Cholleti, L.L. Frye, J.R. Greenwood, M.R. Timlin, M. Uchimaya, Epik: a software program for pK a prediction and protonation state generation for drug-like molecules, J. Comput. Aided Mol. Des. 21 (2007) 681–691, https://doi.org/10.1007/s10822-007-9133-z.
[74] J.R. Greenwood, D. Calkins, A.P. Sullivan, J.C. Shelley, Towards the comprehensive, rapid, and accurate prediction of the favorable tautomeric states of drug-like molecules in aqueous solution, J. Comput. Aided Mol. Des. 24 (2010) 591–604, https://doi.org/10.1007/s10822-010-9349-1.
[75] M. Mileni, D.S. Johnson, Z. Wang, D.S. Everdeen, M. Liimatta, B. Pabst, K. Bhattacharya, R.A. Nugent, S. Kamtekar, B.F. Cravatt, K. Ahn, R.C. Stevens, Structure-guided inhibitor design for human FAAH by interspecies active site conversion, Proc. Natl. Acad. Sci. USA 105 (2008) 12820–12824, https://doi.org/10.1073/pnas.0806121105.
[76] Y. Gao, E. Cao, D. Julius, Y. Cheng, TRPV1 structures in nanodiscs reveal mechanisms of ligand and lipid action, Nature 534 (2016) 347–351, https://doi.org/10.1038/nature17964.
[77] C.-H. Ngan, D.R. Hall, B. Zerbe, L.E. Grove, D. Kozakov, S. Vajda, FTSite: high accuracy detection of ligand binding sites on unbound protein structures, Bioinformatics 28 (2012) 286–287, https://doi.org/10.1093/bioinformatics/btr651.
[78] R.A. Friesner, J.L. Banks, R.B. Murphy, T.A. Halgren, J.J. Klicic, D.T. Mainz, M. P. Repasky, E.H. Knoll, M. Shelley, J.K. Perry, D.E. Shaw, P. Francis, P.S. Shenkin, Glide: a new approach for rapid, accurate docking and scoring. 1. Method and assessment of docking accuracy, J. Med. Chem. 47 (2004) 1739–1749, https://doi.org/10.1021/jm0306430.
[79] T.A. Halgren, R.B. Murphy, R.A. Friesner, H.S. Beard, L.L. Frye, W.T. Pollard, J. L. Banks, Glide: a new approach for rapid, accurate docking and scoring. 2. Enrichment factors in database screening, J. Med. Chem. 47 (2004) 1750–1759, https://doi.org/10.1021/jm030644s.
[80] R.A. Friesner, R.B. Murphy, M.P. Repasky, L.L. Frye, J.R. Greenwood, T. A. Halgren, P.C. Sanschagrin, D.T. Mainz, Extra precision glide: docking and scoring incorporating a model of hydrophobic enclosure for protein−ligand complexes, J. Med. Chem. 49 (2006) 6177–6196, https://doi.org/10.1021/jm051256o.
[81] S. Salentin, S. Schreiber, V.J. Haupt, M.F. Adasme, M. Schroeder, PLIP: fully automated protein–ligand interaction profiler, Nucleic Acids Res. 43 (2015) W443–W447, https://doi.org/10.1093/nar/gkv315.
[82] W. Humphrey, A. Dalke, K. Schulten, VMD: visual molecular dynamics, J. Mol. Graph 14 (1996) 33–38, https://doi.org/10.1016/0263-7855(96)00018-5.
[83] J.Z. Bakdash, L.R. Marusich, Repeated measures correlation, Front. Psychol. 8 (2017), https://doi.org/10.3389/fpsyg.2017.00456.
[84] D. AlKhelb, A. Kirunda, T.C. Ho, A. Makriyannis, R.I. Desai, Effects of the cannabinoid CB1-receptor neutral antagonist AM4113 and antagonist/inverse agonist rimonabant on fentanyl discrimination in male rats, Drug Alcohol Depend. 240 (2022) 109646, https://doi.org/10.1016/j.drugalcdep.2022.109646.
[85] B.J. Neves, M. Mottin, J.T. Moreira-Filho, B.K. de, P. Sousa, S.S. Mendonca, C. H. Andrade, Best practices for docking-based virtual screening, in: Molecular Docking for Computer-Aided Drug Design, Elsevier, 2021, pp. 75–98, https://doi.org/10.1016/B978-0-12-822312-3.00001-1.

[86] A.L. Hopkins, G.M. Keserü, P.D. Leeson, D.C. Rees, C.H. Reynolds, The role of ligand efficiency metrics in drug discovery, Nat. Rev. Drug Discov. 13 (2014) 105–121, https://doi.org/10.1038/nrd4163.
[87] T. Hua, K. Vemuri, S.P. Nikas, R.B. Laprairie, Y. Wu, L. Qu, M. Pu, A. Korde, S. Jiang, J.-H. Ho, G.W. Han, K. Ding, X. Li, H. Liu, M.A. Hanson, S. Zhao, L. M. Bohn, A. Makriyannis, R.C. Stevens, Z.-J. Liu, Crystal structures of agonist-bound human cannabinoid receptor CB1, Nature 547 (2017) 468–471, https://doi.org/10.1038/nature23272.
[88] V. Silva Pereira, B. Elfving, S.R.L. Joca, G. Wegener, Ketamine and aminoguanidine differentially affect Bdnf and Mtor gene expression in the prefrontal cortex of adult male rats, Eur. J. Pharmacol. 815 (2017) 304–311, https://doi.org/10.1016/j.ejphar.2017.09.029.
[89] D.J. Marcus, G. Bedse, A.D. Gaulden, J.D. Ryan, V. Kondev, N.D. Winters, L. E. Rosas-Vidal, M. Altemus, K. Mackie, F.S. Lee, E. Delpire, S. Patel, Endocannabinoid signaling collapse mediates stress-induced amygdalo-cortical strengthening, e6, Neuron 105 (2020) 1062–1076, https://doi.org/10.1016/j.neuron.2019.12.024.
[90] T.M. Eriksson, P. Delagrange, M. Spedding, M. Popoli, A.A. Mathé, S.O. Ögren, P. Svenningsson, Emotional memory impairments in a genetic rat model of depression: involvement of 5-HT/MEK/Arc signaling in restoration, Mol. Psychiatry 17 (2012) 173–184, https://doi.org/10.1038/mp.2010.131.
[91] K.N. Hascup, E.R. Hascup, M.L. Stephens, P.E. Glaser, T. Yoshitake, A.A. Mathé, G.A. Gerhardt, J. Kehr, Resting glutamate levels and rapid glutamate transients in the prefrontal cortex of the flinders sensitive line rat: a genetic rodent model of depression, Neuropsychopharmacol 36 (2011) 1769–1777, https://doi.org/10.1038/npp.2011.60.
[92] L.B. Domingos, H.K. Müller, N.R. da Silva, M.D. Filiou, A.L. Nielsen, F. S. Guimarães, G. Wegener, S. Joca, Repeated cannabidiol treatment affects neuroplasticity and endocannabinoid signaling in the prefrontal cortex of the Flinders Sensitive Line (FSL) rat model of depression, Neuropharmacol 248 (2024) 109870, https://doi.org/10.1016/j.neuropharm.2024.109870.
[93] S. Thiele, T.S. Spehl, L. Frings, F. Braun, M. Ferch, A.H. Rezvani, L.L. Furlanetti, P. T. Meyer, V.A. Coenen, M.D. Döbrössy, Long-term characterization of the Flinders Sensitive Line rodent model of human depression: Behavioral and PET evidence of a dysfunctional entorhinal cortex, Behav. Brain Res. 300 (2016) 11–24, https://doi.org/10.1016/j.bbr.2015.11.026.
[94] R.J. Bluett, R. Báldi, A. Haymer, A.D. Gaulden, N.D. Hartley, W.P. Parrish, J. Baechle, D.J. Marcus, R. Mardam-Bey, B.C. Shonesy, Md.J. Uddin, L.J. Marnett, K. Mackie, R.J. Colbran, D.G. Winder, S. Patel, Endocannabinoid signalling modulates susceptibility to traumatic stress exposure, Nat. Commun. 8 (2017) 14782, https://doi.org/10.1038/ncomms14782.
[95] N.B. Worley, M.N. Hill, J.P. Christianson, Prefrontal endocannabinoids, stress controllability and resilience: a hypothesis, Prog. Neuropsychopharmacol. Biol. Psychiatry 85 (2018) 180–188, https://doi.org/10.1016/j.pnpbp.2017.04.004.
[96] R.J. McLaughlin, M.N. Hill, F.R. Bambico, K.L. Stuhr, G. Gobbi, C.J. Hillard, B. B. Gorzalka, Prefrontal cortical anandamide signaling coordinates coping responses to stress through a serotonergic pathway, Eur. Neuropsychopharmacol. 22 (2012) 664–671, https://doi.org/10.1016/j.euroneuro.2012.01.004.
[97] C. Kirkedal, G. Wegener, F. Moreira, S.R.L. Joca, N. Liebenberg, A dual inhibitor of FAAH and TRPV1 channels shows dose-dependent effect on depression-like behaviour in rats, Acta Neuropsychiatr. 29 (2017) 324–329, https://doi.org/10.1017/neu.2016.68.
[98] S.F. de Boer, B. Buwalda, J.M. Koolhaas, Untangling the neurobiology of coping styles in rodents: towards neural mechanisms underlying individual differences in disease susceptibility, Neurosci. Biobehav. Rev. 74 (2017) 401–422, https://doi.org/10.1016/j.neubiorev.2016.07.008.
[99] A. Ramos, P. Mormède, Stress and emotionality: a multidimensional and genetic approach, Neurosci. Biobehav. Rev. 22 (1997) 33–57, https://doi.org/10.1016/S0149-7634(97)00001-8.
[100] L. Lindgren, S. Gouveia-Figueira, M.L. Nording, C.J. Fowler, Endocannabinoids and related lipids in blood plasma following touch massage: a randomised, crossover study, BMC Res. Notes 8 (2015), https://doi.org/10.1186/s13104-015-1450-z.
[101] A. Lama, C. Pirozzi, C. Annunziata, M.G. Morgese, M. Senzacqua, I. Severi, A. Calignano, L. Trabace, A. Giordano, R. Meli, G. Mattace Raso, Palmitoylethanolamide counteracts brain fog improving depressive-like behaviour in obese mice: possible role of synaptic plasticity and neurogenesis, Br. J. Pharmacol. 178 (2021) 845–859, https://doi.org/10.1111/bph.15071.
[102] F. Guida, L. Luongo, F. Marmo, R. Romano, M. Iannotta, F. Napolitano, C. Belardo, I. Marabese, A. D'Aniello, D. De Gregorio, F. Rossi, F. Piscitelli, R. Lattanzi, A. De Bartolomeis, A. Usiello, V. Di Marzo, V. De Novellis, S. Maione, Palmitoylethanolamide reduces pain-related behaviors and restores glutamatergic synapses homeostasis in the medial prefrontal cortex of neuropathic mice, Mol. Brain 8 (2015), https://doi.org/10.1186/s13041-015-0139-5.
[103] M.N. Hill, W.S.V. Ho, C.J. Hillard, B.B. Gorzalka, Differential effects of the antidepressants tranylcypromine and fluoxetine on limbic cannabinoid receptor binding and endocannabinoid contents, J. Neural Transm. 115 (2008) 1673–1679, https://doi.org/10.1007/s00702-008-0131-7.
[104] I. Smaga, B. Bystrowska, D. Gawliński, B. Pomierny, P. Stankowicz, M. Filip, Antidepressants and changes in concentration of endocannabinoids and N-acylethanolamines in rat brain structures, Neurotox. Res. 26 (2014) 190–206, https://doi.org/10.1007/s12640-014-9465-0.
[105] I. Smaga, B. Bystrowska, D. Gawliński, B. Pomierny, P. Stankowicz, M. Filip, Antidepressants and changes in concentration of endocannabinoids and N-acylethanolamines in rat brain structures, Neurotox. Res. 26 (2014) 190–206, https://doi.org/10.1007/s12640-014-9465-0.
[106] A. Sharafi, S. Pakkhesal, A. Fakhari, N. Khajehnasiri, A. Ahmadalipour, Rapid treatments for depression: endocannabinoid system as a therapeutic target, Neurosci. Biobehav. Rev. 137 (2022) 104635, https://doi.org/10.1016/j.neubiorev.2022.104635.
[107] J. Dragon, E. Obuchowicz, How depression and antidepressant drugs affect endocannabinoid system?—review of clinical and preclinical studies, Naunyn Schmiede Arch. Pharmacol. 397 (2024) 4511–4536, https://doi.org/10.1007/s00210-023-02938-z.
[108] A.R. Tejeda-Martínez, J.M. Viveros-Paredes, G.V. Hidalgo-Franco, E. Pardo-González, V. Chaparro-Huerta, R.E. González-Castañeda, M.E. Flores-Soto, Chronic inhibition of FAAH reduces depressive-like behavior and improves dentate gyrus proliferation after chronic unpredictable stress exposure, Behav. Neurol. 2021 (2021) 1–14, https://doi.org/10.1155/2021/6651492.
[109] I. Gallego-Landin, A. García-Baos, A. Castro-Zavala, O. Valverde, Reviewing the role of the endocannabinoid system in the pathophysiology of depression, Front. Pharmacol. 12 (2021), https://doi.org/10.3389/fphar.2021.762738.
[110] U. Bright, I. Akirav, Modulation of endocannabinoid system components in depression: pre-clinical and clinical evidence, Int. J. Mol. Sci. 23 (2022) 5526, https://doi.org/10.3390/ijms23105526.
[111] R.J. McLaughlin, M.N. Hill, F.R. Bambico, K.L. Stuhr, G. Gobbi, C.J. Hillard, B. B. Gorzalka, Prefrontal cortical anandamide signaling coordinates coping responses to stress through a serotonergic pathway, Eur. Neuropsychopharmacol. 22 (2012) 664–671, https://doi.org/10.1016/j.euroneuro.2012.01.004.
[112] F.A. Moreira, Serotonin, the prefrontal cortex, and the antidepressant-like effect of cannabinoids, J. Neurosci. 27 (2007) 13369–13370, https://doi.org/10.1523/JNEUROSCI.4867-07.2007.
[113] F.R. Bambico, N. Katz, G. Debonnel, G. Gobbi, Cannabinoids elicit antidepressant-like behavior and activate serotonergic neurons through the medial prefrontal cortex, J. Neurosci. 27 (2007) 11700–11711, https://doi.org/10.1523/JNEUROSCI.1636-07.2007.
[114] J. Sowa, M. Kusek, B. Bobula, G. Hess, K. Tokarski, Ketamine administration reverses corticosterone-induced alterations in excitatory and inhibitory transmission in the rat dorsal raphe nucleus, Neural Plast. 2019 (2019) 1–10, https://doi.org/10.1155/2019/3219490.
[115] L.B. Domingos, N.R. Silva, A.J.M. Chaves Filho, A.J. Sales, A. Starnawska, S. Joca, Regulation of DNA methylation by cannabidiol and its implications for psychiatry: new insights from in vivo and in silico models, Genes (Basel) 13 (2022), https://doi.org/10.3390/genes13112165.
[116] T. Nguyen, J. Li, B.F. Thomas, J.L. Wiley, T.P. Kenakin, Y. Zhang, Allosteric modulation: an alternate approach targeting the cannabinoid CB1 receptor, Med. Res. Rev. 37 (2017) 441–474, https://doi.org/10.1002/med.21418.
[117] I. Smaga, M. Zaniewska, D. Gawliński, A. Faron-Górecka, P. Szafrański, M. Cegła, M. Filip, Changes in the cannabinoids receptors in rats following treatment with antidepressants, Neurotoxicology 63 (2017) 13–20, https://doi.org/10.1016/j.neuro.2017.08.012.
[118] F.R. Bambico, G. Gobbi, The cannabinoid CB1 receptor and the endocannabinoid anandamide: possible antidepressant targets, Expert Opin. Ther. Targets 12 (2008) 1347–1366, https://doi.org/10.1517/14728222.12.11.1347.
[119] V. Micale, V. Di Marzo, A. Sulcova, C.T. Wotjak, F. Drago, Endocannabinoid system and mood disorders: priming a target for new therapies, Pharmacol. Ther. 138 (2013) 18–37, https://doi.org/10.1016/j.pharmthera.2012.12.002.
[120] M.N. Hill, W.-S.V. Ho, C.J. Hillard, B.B. Gorzalka, Differential effects of the antidepressants tranylcypromine and fluoxetine on limbic cannabinoid receptor binding and endocannabinoid contents, J. Neural Transm. 115 (2008) 1673–1679, https://doi.org/10.1007/s00702-008-0131-7.
[121] A.A. Rey, M. Purrio, M.-P. Viveros, B. Lutz, Biphasic effects of cannabinoids in anxiety responses: CB1 and GABAB receptors in the balance of GABAergic and glutamatergic neurotransmission, Neuropsychopharmacology 37 (2012) 2624–2634, https://doi.org/10.1038/npp.2012.123.
[122] A.L.B. Terzian, V. Micale, C.T. Wotjak, Cannabinoid receptor type 1 receptors on <scp>GABA</scp> ergic vs. glutamatergic neurons differentially gate sex-dependent social interest in mice, Eur. J. Neurosci. 40 (2014) 2293–2298, https://doi.org/10.1111/ejn.12561.
[123] R. Ettaro, L. Laudermilk, S.D. Clark, R. Maitra, Behavioral assessment of rimonabant under acute and chronic conditions, Behav. Brain Res. 390 (2020), https://doi.org/10.1016/j.bbr.2020.112697.
[124] G. Griebel, J. Stemmelin, B. Scatton, Effects of the cannabinoid CB1 receptor antagonist rimonabant in models of emotional reactivity in rodents, Biol. Psychiatry 57 (2005) 261–267, https://doi.org/10.1016/j.biopsych.2004.10.032.
[125] D. Rafiei, N.J. Kolla, Molecular sciences elevated brain fatty acid amide hydrolase induces depressive-like phenotypes in rodent models: a review, Rev. Int. J. Mol. Sci. (2021), https://doi.org/10.3390/ijms2203.
[126] M. Häring, V. Enk, A.A. Rey, S. Loch, I.R. de Azua, T. Weber, D. Bartsch, K. Monory, B. Lutz, Cannabinoid type-1 receptor signaling in central serotonergic neurons regulates anxiety-like behavior and sociability, Front. Behav. Neurosci. 9 (2015), https://doi.org/10.3389/fnbeh.2015.00235.
[127] F.R. Bambico, N. Katz, G. Debonnel, G. Gobbi, Cannabinoids elicit antidepressant-like behavior and activate serotonergic neurons through the medial prefrontal cortex, J. Neurosci. 27 (2007) 11700–11711, https://doi.org/10.1523/JNEUROSCI.1636-07.2007.
[128] S. Haj-Dahmane, R.-Y. Shen, Modulation of the serotonin system by endocannabinoid signaling, Neuropharmacology 61 (2011) 414–420, https://doi.org/10.1016/j.neuropharm.2011.02.016.
[129] X. López-Gil, L. Jiménez-Sánchez, L. Campa, E. Castro, C. Frago, A. Adell, Role of serotonin and noradrenaline in the rapid antidepressant action of ketamine, ACS

Chem. Neurosci. 10 (2019) 3318–3326, https://doi.org/10.1021/acschemneuro.9b00288.

[130] K. Fukumoto, M. Iijima, T. Funakoshi, S. Chaki, Role of 5-HT1A receptor stimulation in the medial prefrontal cortex in the sustained antidepressant effects of ketamine, Int. Int. J. Neuropsychopharmacol. 21 (2018) 371–381, https://doi.org/10.1093/ijnp/pyx116.

[131] J.E. Ortega, V. Gonzalez-Lira, I. Horrillo, M. Herrera-Marschitz, L.F. Callado, J. J. Meana, Additive effect of rimonabant and citalopram on extracellular serotonin levels monitored with in vivo microdialysis in rat brain, Eur. J. Pharmacol. 709 (2013) 13–19, https://doi.org/10.1016/j.ejphar.2013.03.043.